FINITE ELEMENT MODELLING FOR EVALUATION OF COMPRESSION/RELEASE STABILIZED TRANSFEMORAL PROSTHETIC SOCKET

MENG ZHAOJIAN

MPhil

The Hong Kong Polytechnic University

2019

The Hong Kong Polytechnic University

Department of Biomedical Engineering

Finite Element Modelling for Evaluation of Compression/Release Stabilized Transfemoral Prosthetic Socket

MENG ZHAOJIAN

A thesis submitted in partial fulfillment of the requirements for

the degree of Master of Philosophy

January 2018

CERTIFICATE OF ORIGINALITY

I hereby declare that this thesis is my own work and that, to the best of my knowledge and belief, it reproduces no material previously published or written, nor material that has been accepted for the award of any other degree or diploma, except where due acknowledgement has been made in the text.

_____ Singed

MENG Zhaojian (Name of student)

ABSTRACT

Amputees who lost their lower limbs are mostly fitted with prostheses to facilitate standing and locomotion. Prosthetic socket, which is the direct contact and interaction of the prosthesis with the residual limb as the crucial element that influences the quality of prosthesis fitting. Transfemoral amputees complain pain, abrasion, humidity, inconvenient donning and doffing, and poor control of prosthesis with conventional socket designs. The newly developed compression/release stabilized (CRS) concept has the aim to increase the prosthetic socket control efficiency and stability through pre-compressing the residual limb surface along the shaft of the bone. In transfemoral CRS prosthetic socket design, four longitudinal depressions pre-compress on soft tissue along the femoral bone to stabilize the residual limb and four release areas adjacent to the compressed parts allow tissues to displace. The Further motion of the bone within the soft tissues is minimized with this pre-compression. The momentum directly transfers through the compressed thigh muscle to the socket without soft tissues motion. There is no need to have a proximal socket brim because the residual limb is better controlled, and more weight is supported along the femoral shaft. However, there are little publications and investigation on the transfemoral CRS prosthetic socket design. This study aimed to better understand the stress and strain distribution of the transfemoral residual limb inside transfemoral CRS socket by finite element method.

A pilot study was conducted to fit a trial prosthetic socket on a healthy subject and a transfemoral amputee to find an appropriate reference for the geometry of the compression areas of the CRS socket design. An FE model of the transfemoral residual limb was established from the MR image of the transfemoral subject. The CRS socket design was constructed by using the 3D reconstructed geometry of the residual limb to increase the accuracy of the assembled FE models. Two stages were performed in this study: first, the CRS socket model underwent 106mm displacement (which was vertical displacement of the residual limb from just in touch with socket to the fully donned position) to simulate the donning procedure; second, an 800N force was applied as the subject's total body weight on the femoral head to exam the loading effect. The baseline of the compression value was set as 15mm derived from the pilot study on the evaluation of different compression depth. For comparison, a CRS socket with 10mm compression was constructed as well. The FE results were validated experimentally with interface pressure measurement. The effects of material with a different coefficient of friction (0.3, 0.4 and 0.5) and the inclusion of silicone liner were simulated by the FE model.

The results showed that the maximum FE predicted normal pressure was 212 kPa in the proximal anterior-medial side of residual limb surface. It was higher than the recent literature on the transfemoral study which indicated that the further compression in CRS socket design achieved. When the simulated coefficient of friction was reduced from 0.5 to 0.4 and then 0.4 to 0.3, the maximum contact pressure was reduced 26.73% and 2.56% respectively. When the depth of the compression areas was decreased from 15mm to 10mm, the maximum contact pressure in the donning and loading conditions were reduced by 14.68% and 7.78%

respectively. With a 3mm thick silicone liner, there was much about 40% maximum pressure reduction.

The patient responded positively with the CRS socket design in this study. This method may help the prosthetist to design the CRS socket more accurate and faster.

PUBLICATIONS ARISING FROM THE THESIS

Conference and Journal Paper

Meng, Z.J., Leung, A.K.L. Effect of SACH Foot and Single Axis Foot on The Walking Stability of Transtibial Amputees. Asian Prosthetic and Orthotic Scientific Meeting 2016, Seoul, South Korea, Nov. 4th to 6th 2016.

Meng, Z.J., Zhang, M., & Leung, A.K.L., A novel method to design a compression release stabilized prosthetic socket. International Rehabilitation Canton Forum 2018, Guangzhou, April 2nd to 4th 2018. Best paper award: 2nd runner-up.

Meng, Z.J., Zhang, M., &Leung, A.K.L. Finite Element Evaluation of Compression/Release Stabilized Transfemoral Socket Effect on Residual limb. Asian Prosthetic and Orthotic Scientific Meeting 2018, Bangkok, Thailand, Nov. 6th to 9th 2018.

Meng, Z.J., Wong, D.W.C, Zhang, M., & Leung, A.K.L., Analysis of Compression/Release Stabilized Transfemoral Prosthetic Socket by Finite Element Modelling. (Submitted)

ACKNOWLEDGEMENTS

I would like to express my great gratitude to my supervisor Dr. Aaron K.L. Leung for his patient supervision and guidance, especially for his support during the hard time. I am thankful to Co-supervisor Prof. Ming Zhang for his kind support in this project. I would like to thank Dr. M. S. Wong for his constructive comments and recommendations on the thesis.

Special thanks to Mr. Yan Fei for providing me the CT image to construct FE model for pilot study. My special thanks also go to Mr. Li Ning who gave me valuable suggestions and feedback in the casting and socket evaluation process. I would like to thanks to Mr. Duo Wong Wai-chi and Miss. Wang Yan who helped me in the learning and using of the FE method, and Mr. Hassan Beygi Babak, Miss Lin Yangmin, Mr. Chris, Leung Tsz Kin in the 3D scanning and design process.

I would like to deliver my gratitude to Mr. Li Ho Yip who provided support for me in the laboratory setup, as well as Mr. Alex Auyang Lau and Mr. Ajax Lau of the Prince of Wales Hospital (PWH) for their facilitating of using CAD-CAM approach to fabricate positive models for CRS socket fabrication.

I would like to thanks Dr. Daniel Wu and Ms. Rachel Tam of the Center for Dr. Wu's Bunion Surgery for the arrangement of MRI imaging process.

During this project, I have developed perseverance, endurance, and self-discipline. I appreciate myself that I have overcome many difficulties.

Finally, the most important thanks go to my beloved family: my wife and son for their unconditionally support; my sister and brother-in-law who have been taking care my great Mom since she has injured. This work cannot be accomplished without their love and encouragement.

TABLE OF CONTENTS

LIST OF FIGURES

List of tables

List of abbreviations

CRS: Compression/release stabilized

CAD: Computer-aided design

CAM: Computer-aided manufacturing

Quad: Quadrilateral

FE: Finite element

IRC: Ischial-ramal containment

NSNA: Normal shape normal alignment

UCLA: University California, Los Angeles

CAT-CAM: Contoured adducted trochanteric – Controlled alignment method

OI: Osseointegration

2D: Two dimension

3D: Three dimension

FEM: Finite element method

OPRA: Osseointegrated prosthesis for rehabilitation of amputees

PEQ: Prosthesis evaluation questionnaire

VAS: Visual analogue scoring

CHAPTER 1 INTRODUCTION

1.1 Amputation-prevalence and problems

Losing the extremities hinders people to perform daily activities. The tasks such as cooking, eating, washing face challenge the upper limb amputees. Lower limb amputation, on the other hand, affects the locomotion. The leading causes of amputations are vascular disease, trauma, malignancy, and congenital limb deficiencies (Ephraim et al., 2003).

Through the year 1988 to 1996, there were 133,235 limb deficiencies per year in which 82% of limb-loss caused by the vascular disorder. The percentage raised from 38.3 per 100,000 population in 1988, to 46.19 per 100,000 population in 1996. Trauma, the second cause of amputations accounted for 11.37 per 100,000 population decreased to 5.86 per 100,000 population in 1996. The lower limb accounted for 53.6% dysvascular amputation. The transfemoral was 25.8% and 27.6% for the transtibial amputation (Dillingham et al., 2002). The lower limb amputation was increased to over 80% of amputee population (Dillingham et al., 2016). The amputee population was predicted to reach 3.6 million by the year 2050 in the US (Ziegle-Grahm, 2008). The incidence of amputation was 5.1 per 100,000 population from the year 2003 to 2008 in England (Moxey et al., 2010).

Most of the amputees suffered not only phantom limb pain, residual limb pain, and back pain but also experienced extra financial burden (Smith et al., 1999). The cost related to fitting a prosthesis for five-year care was much higher than an average person's lifetime health care costs (Sheehan, 2014).

Adaptation to the amputation was an essential factor of rehabilitation. Psychological depression and anxiety were developed after the amputation. The amputees may have 18-20 months of depression and extend to 10 to 20 years, or even for the whole life (Horgan & MacLachlan, 2014). An immediate post-rehabilitation is a crucial process to reduce such syndrome. These include prosthetic fitting, multi-disciplinary team rehabilitation, mobilization, and physiotherapy.

Up to 41% of the lower limb amputees encountered skin problems in their residual limb. This attributed to inappropriate interaction of the residual limb with the prosthetic socket (Bui, 2009; Uustal, 2014). Transfemoral amputees were found to be less satisfied with their prosthetic socket than transtibial counterparts (Turney, 2001). It is likely caused by the inappropriate pressure and stress produced inside the socket. Therefore, it was important to have the socket structure, which could maximize the tolerable compression areas and offload the pressure sensitive regions on the residual limb surface (Yoo, 2014).

By direct attaching the external prosthesis with the residual limb bone, the osseointegration prosthesis enhances prosthetic control efficiency. The walking performance and prosthesis-related quality of life were improved as well (Van de Meent, 2013). However, the potential high risk of infection, especially in areas with high temperature, falling fracture, and humidity prevent the wide application of this method.

1.2 Background

After lower limb amputation, a prosthesis is usually prescribed for the patient to facilitated standing and locomotion. In general, the amputee's functions are affected by the level of amputation. The more proximal the amputation, the more barriers the amputee suffers. Compared with transtibial amputation, the situation for the transfemoral case was worse because of the loss of the knee joint (Gottschalk & Stills, 1994). The physiological energy expenditure is a useful predictor to measure the patient functional performance (Waters & Mulroy, 1999). The study found the energy consumption for a transfemoral amputee could reach 65% higher than healthy subjects at level walking (Waters et al., 1976). A significant reduction of oxygen consumption was shown during walking for transtibial amputee compared with the transfemoral one (Huang et al., 1979). A typical lower limb prosthesis contains the socket, prosthetic joint, prosthetic foot, and auxiliary components. Besides the amputee's health condition, there are many factors to influence the outcome of prosthesis fitting. Using different prosthetic components affects functional outcome. With the advanced technology, a lot of research efforts were put on the development of prosthetic components such as computerized prosthetic knee joint, energy storage foot. Microprocessor or external power is applied to prosthetic design to neutralize the gait; numerous carbon prosthetic feet are designed to restore and release energy. All of these try to lower the energy consumption and improve biological function (Buckley et al., 1997; Schamalz et al., 2002; Versluys, 2009). The gait pattern and energy consumption have been benefiting from these emerging technologies. Many advanced prosthetic joints and feet have been available in the market. However, the most important part of a successful prosthetic fitting is the prosthetic socket.

The prosthetic socket directly encompasses the residual limb and connects the external parts: adaptor, pylon, a prosthetic foot and joint. It provides prosthesis suspension and body loading transfer. It is quite often patients refuse to use a prosthesis while the prosthetic socket cannot fit him/her well. The common problems on the residual limb caused by the socket include ulcers, irritations, and skin problems such as inclusion cysts, calluses, verrucous hyperplasia and allergic contact dermatitis (Dudek et al., 2006; Dudek et al., 2005). Excessive shear force, humidity, and pressure between the residual limb and socket can all be the causes (Lyon et al., 2000). Residual limb pain and discomfort caused by the prosthetic socket reduces the utilization of prosthesis (Meulenbel et al., 2011; Nielsen, 1991).

The quadrilateral socket (Quad) socket and ischial-ramal containment (IRC) socket are the conventional transfemoral prosthetic socket types which have been adopted for many decades. The Quad socket has a quadrilateral brim that is narrower in the anterior-posterior direction compared to the medial-lateral direction. The ischial tuberosity rests on the posterior brim for weight-bearing and force transfer (Radcliffe, 1955). Since there is no bony lock to secure the ischium, the pelvis may shift medially during weight bearing and increase residual femur abduction. This may lead to increased discomfort at the distal end of the residual limb and lateral lurch of the amputated limb. These problems were addressed by the ischial-ramal containment (IRC) socket developed in the 1980s (Long, 1975; Schuch, 1987; Sabolich, 1985). The IRC socket extends the posteromedial brim of the socket to support the medial border of the ischial tuberosity and ramus by an oblique and sloping contours design. Compared with the Quad socket, it is narrower in the medial-lateral dimension (Schuch and Pritham, 1999). The Quad and IRC share similar design features, and both reduce the hip range of motion (Klotz et al., 2011; Hagberg et al., 2005). The IRC socket design has been

further improved and is referred to the Marlo Anatomical Socket (MAS). Instead of containing the ischium, the MAS surrounds the ischio-pubic ramus but allows a release on the posterior gluteal portion. Improved comfort, stability and reduced energy cost of walking were reported (Trower, 2006; Traballesi et al., 2011).

The findings of previous studies indicate that the muscle and fat in the prosthetic socket are compressed first as the residual limb operates the prosthesis (Alley et al., 2011). This compression causes the motion lost which compromises the control efficiency and stability. Although the MAS and IRC socket result in better prosthetic control compared to the Quad socket, it remains challenging to reduce the lost motion induced by muscle and fat compression between the residual limb bone and prosthetic socket. To minimize the motion lost, the compression/release stabilization (CRS) socket design approach was recently introduced. In the transfemoral CRS socket, there are four longitudinal pre-compression bars along femur to stabilize the bone, and four release regions adjacent to the compression bars to allow some soft tissue movement. Momentum is directly transferred through the thigh to the socket with little motion of soft tissues (Alley and Williams, 2012; Paterno et al., 2017). There may be no need for a more proximal socket when the thigh is better controlled, accordingly increase the hip range of motion. The control stability, sitting, donning and doffing comfort may be improved by the CRS structure (Paterno et al., 2018; Cutler, 2017). However, the condition of the residual limb under further compression is not clear.

The procedure for the prosthetic treatment to an amputee starts from examination, treatment plan, measurement and casting, plaster cast rectification, fabrication, fitting and evaluation. It is a time-consuming process. With the advancement of computer technology, there have been alternatives for some of the manual process in prosthetics service. Computer-aided design (CAD), and computer-aided manufacturing (CAM) were first attempted in the provision of the prosthetic socket in the 1960s. The CAD/CAM has shortened the delivery time and made the product reproducible (Klasson, 1985). Although the process is accelerated by employing the CAD/CAM, the design and modification have to rely on practitioners' experience. It was more convenient and accurate if we could test the P&O products through a simulation process before we apply it to patients. The Finite element simulation is an option. The prosthetic socket fitting process is optimized by employing the finite element analysis in the CAD/CAM system (Figure 1.1). The service team can apply FE simulation process of the prosthetic socket design before using CAM or 3D printing process to fabricate the socket (Zhang et al., 1998). This study aimed to evaluate the pressure and stress distribution on the transfemoral residual limb using the CRS socket by the finite element (FE) method. The simulation results have the potential to guide transfemoral CRS socket design.

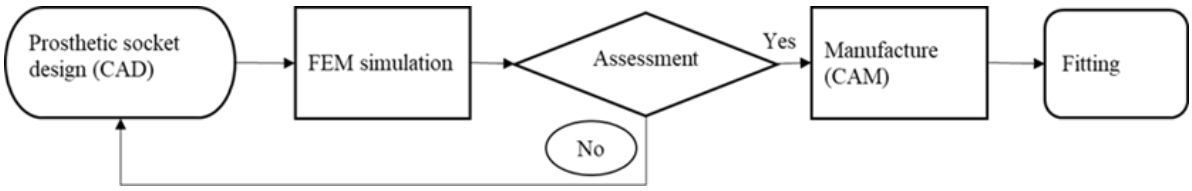

Figure 1.1 Flowchart of socket design with CAD-CAM (Zhang et al., 1998)

1.3 Objective of this study

Compression/Release Stabilized (CRS) transfemoral prosthetic socket design is relatively new. Scientific understanding of the CRS approach is necessary for a positive outcome of socket fitting. The study hypotheses were:

- The CRS socket increases the pressure on the residual limb surface, and the interfacial pressure between the residual limb and socket is increased with the compression depth;

- The pressure and stress can be adjusted by socket coefficient of friction, and the inclusion of a silicone liner.

The goal of this study was to develop an FE model to evaluate the pressure distribution on the residual limb of the patient that fitted with the CRS socket.

The objectives of this research were:

1. To develop an FE model to evaluate the pressure distribution in the transfemoral prosthetic socket with using a Compression/Release Stabilized (CRS) socket design;
2. To study the effect of compression depth of the CRS socket on residual limb stress distribution;
3. To simulate the effect of socket material with different coefficients of friction and inclusion of a silicone liner on the residual limb stress;

CHAPTER 2 LITERATURE REVIEW

2.1 Transfemoral prosthetic socket design

The history of prosthesis can be traced back to early Egypt. The first discovered prosthesis was an artificial big toe made of wood to accomplish physical integrity. The fixation of the big toe was achieved by tightening the textile lace attached with it (Nerlich et al., 2000). It had been gone for a long time that prosthesis was developing very slow. At an early stage, the prosthetic socket was like a bucket to hold the residual limb and employed a strap crossing over the upper adjacent joint for suspension. The prosthetic knee joint and foot were not functional. The prosthesis was mainly made of iron, steel, leather, copper, and wood. The work was always performed by a skillful craftsman. There was no understanding of human biomechanics and material science. Marks (1860) used a hard rubber foot instead of wooden foot design. Hanger introduced the first articulated prosthetic foot with the rubber bumper as plantarflexion stop (Shurr & Michael, 2002). Pabmelee (1863) first invented suction suspension method for lower limb prosthetic socket. The lower limb prosthesis became more functional. After the World War II, there was a major impetus for the development of the prosthetic industry. Radcliffe (1955) developed the transfemoral quadrilateral (Quad) prosthetic socket which was named by its cross-section view. It is characterized by the narrow anterior-posterior dimensions and the wide medial-lateral dimensions (Radcliffe, 1955). Many transfemoral amputees still use it nowadays.

In quadrilateral socket design, ischial tuberosity and gluteal muscles are sitting at the medial-posterior brim platform for weight bearing and force transfer. There are anatomical relieve channels for muscles and tendons of the thigh. The donning of the prosthesis is like a plug-in action. Ideally, the residual limb is in total contact with the inner surface of the socket to increase contact area and decrease interface pressure. The distal end of residual limb contacts with the bottom of the socket, which did not happen in traditional open-ended design (Hall, 1964). It offers alternative positive and negative pressure during gait to enhance distal residual limb circulation, reduce edema and improve proprioception (Backus, 2005; Bakalima, 1966). Discomfort at the end of the residual limb and lateral lurch to the amputated side during standing and walking were reported. Researchers tried to find out the reasons and mechanism behind. Prosthetist examined the residual femur position inside the socket by X-ray method (Long, 1975). He reported that the femur was abducted inside the quadrilateral socket. The study concluded that quadrilateral socket design was insufficient to control the adduction of femur inside the socket, and subsequently pelvis falling to the sound side.

In erect standing, the femoral shaft of a healthy subject is about 9-degree in adduction. The adductor magnus is the most contributor to the adduction position of the thigh. Nearly 2/3 of adduction moment would be lost if the adductor magnus was amputated (Gottschalk, 1992). The gluteus medius pulls the femur into an abduction position when it is functioning. Because ischium tuberosity is sitting on the medial-posterior seat, there is no bony lock to hold the ischium in a stable position. This causes a medial shift of pelvis and thus increase the femur abduction. As a result, there is excessive pressure on the medial proximal soft tissue and the lateral distal femur. The pain would be generated in these two areas, and lateral lurch happens in the frontal plane (Sabolich, 1985). By placing femur in an adducted position, patients

started to walk in a more narrowed walking width. The balance is improved by setting the prosthetic foot under the hip joint. Long (1985) defined this referencing line the normal shape normal alignment (NSNA). This was achieved by narrowing the medial-lateral dimension of the socket and increasing the anterior-posterior size. Based on Ivan Long's theory and observation, John Soblish from University California, Los Angeles (UCLA) and Daniel Shamp from New York University developed the Contoured Adducted Trochanteric-Controlled Alignment Method (CAT-CAM) and the narrow M-L concept of the transfemoral prosthetic socket respectively. The design is varied; the fundamental concept is similar. It attempts to hold the femur in adduction position by narrowing the M-L dimension and preventing the ischium tuberosity to slide. This kind of socket is classified as ischial-ramal containment (IRC) socket (Pritham, 1988). The structure of Quad and IRC socket with ischial bone shows in Figure 2. 1 a and b. The study found the energy consumption efficiency and gait parameters were improved for IRC socket than Quad socket (Gailey et al., 1993). The evaluation of X-ray on fifty transfemoral subjects fitted either quadrilateral or IRC socket showed that there was no significant in the adduction angle control of femur regarding the socket design (Gottschalk et al., 1989; Schuch, 1999). There were lots of complaints about the poor appearance and constraint of hip range of motion caused by the hard shell of the ischium region of the posterior part of the socket in Quad and IRC socket. Recently, IRC socket was redesigned as the Marlo anatomical socket shape (Fairley, 2004; Ortiz, 2013). It has a lower profile at the posterior ischium part and further extends to ischio-pubic ramus (Figure 2. 2). The range of motion is improved and with better cosmetic.

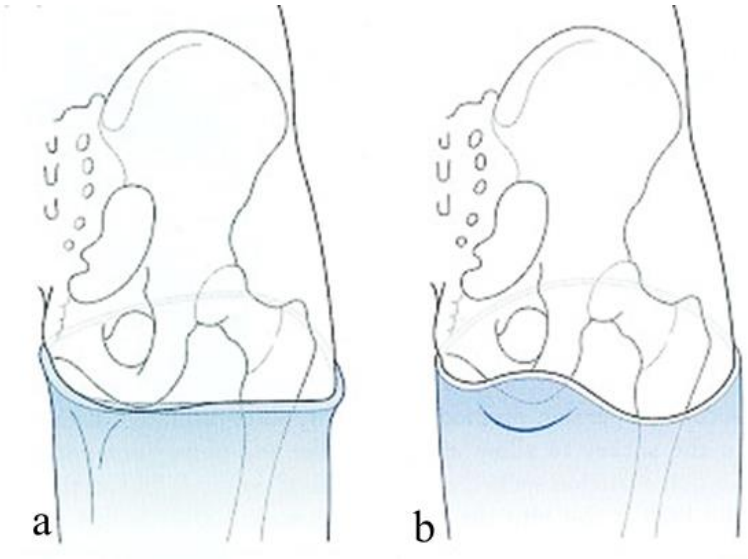

Figure 2. 1 Location of ischium and pelvis for the Quad (a) and IRC socket (b). Retrieved from: http://m.blog.daum.net/jasegood02/26

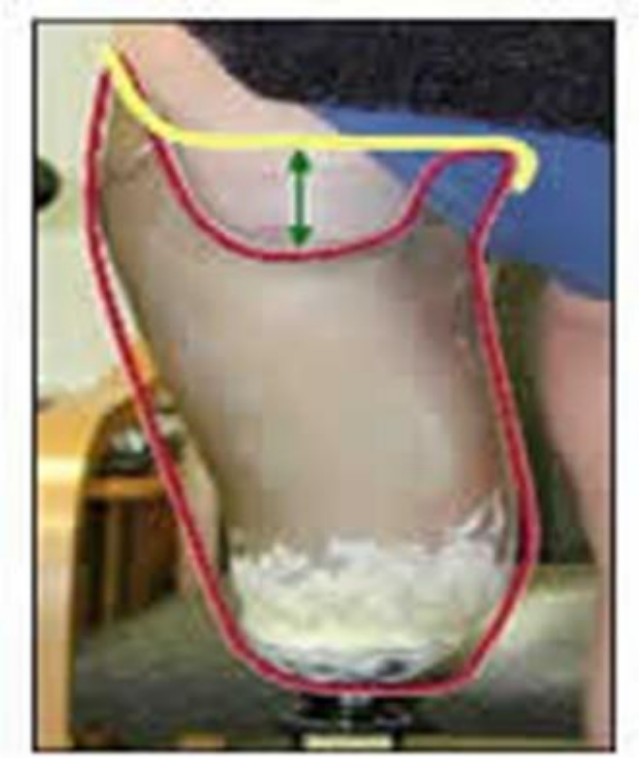

Figure 2. 2 Posterior view of Marlo socket (Pike, 2002)

Over the century, researchers are pursuing the optimum adduction control of residual femur and evaluating the effectiveness of it. The scientist never ignores suspension as another essential function of the socket. The suspension which ensuring the socket does not drop from the residual limb during swing phase was previously achieved by waist strap. The quality of suspension is determined by the method it employed and tightness of socket fit. From the waist strap to suction, gel liners or pin-lock system, the socket suspension has been improved a lot (Meim et al., 1997). It would be excellent if there is no/small relative motion between the residual limb and socket. It is better than the past, but hard to be perfect. Movement between the residual limb and socket induces piston effect if the suspension and tightness of socket are inappropriate. Pain, skin breakdown and insufficient control of prosthesis are the most common phenomena in piston motion (Beil et al., 2002; Eberhart & Mckennon, 1954; Lyon, 2000). A study for 13 transfemoral amputees fitted with IRC and CRS (HiFi) socket found that the walking capacity and balance all improved by the CRS socket (Kahle et al., 2016).

The loose suspension and piston action are well solved by osseointegration, which fixes a titanium implant into the femur bone and attaches external prosthetic components with an abutment. The treatment involves two surgical procedures. The first step is to insert a titanium fixture into the shaft of the femur and requires about six months for the healing process. The next surgery is required after the completion of the healing process. The surgeon uses a fixture to screw a titanium rod penetrating the skin into the bone. The prosthesis is then attached to it (R. Brånemark et al., 2001; Hagberg et al., 2014). More frequent use of the prosthesis, easy donning and doffing, becoming more active and radical functional improvements are the benefit of osseointegrated prosthesis reported. The bone-anchored prosthesis enables the

amputees feeling to regain themselves as before the amputation (Lundberg et al., 2011). The complications are also apparent. These include infection at the skin penetration site, and the potential loosen and bending of the fixation. Additionally, the process is time-consuming, as the whole treatment requires 18 months or a more extended period.

2.2 Transfemoral prosthetic socket suspension

The prosthetic socket design is vital for the amputees. Suspension of the prosthetic socket on the residual limb is another critical factor affecting the quality of the prosthetic intervention. Ideally, there should be no relative motion between the prosthetic socket and the residual limb. However, it is hard to achieve. There is always relative motion between the residual limb and socket as well as any interface between two. It will induce the piston effect if the suspension is not strong enough. Amputees complained of pain and skin breakdown. Therefore, a good suspension system is essential for good socket fitting (Beil et al., 2002; Eberhart & McKennon, 1954; Lenze & Del Rossi, 1994). The waist belt was early stage suspension, which the elastic strap connected with socket and encircled the pelvis between the iliac crests and the greater trochanter (Figure 2. 3).

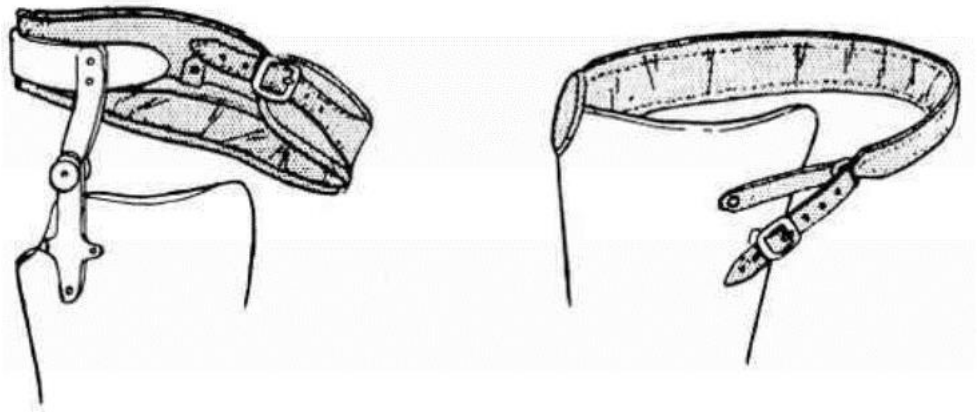

Figure 2. 3 Left, the Silesian belt. Right the waist belt (Muller, 2016)

One of the most widely used suspensions is suction. The suction suspension uses the surface tension, negative pressure, and muscle contraction. It increases the range of motion and achieves better appearance than the waist belt. The patients use elastic bandages or slip socks surrounding the residual limb first; then, pull the limb into the socket. When all the soft tissue smoothly inside the socket, the prosthetic socket is sealed from the distal medial end by a one-way expulsion valve (Figure 2.4, Left). The negative pressure inside the socket makes the socket well held with residual limb. Excessive tissue rolls between the upper socket brim and pelvis are always the consequence of improper donning. The patient feels uncomfortable or painful when this occurs. Therefore, the training on donning suction type prosthesis is necessary for a proper fitting. Sometimes, the auxiliary suspension belts are connected to the suction socket to increase prosthetic control when the patient's residual limb is too short.

Figure 2. 4 Left, a suction socket with nylon slip socks; Middle, gel liners with a pin lock or a lanyard system; Right, seal-in liner (Carroll, 2006; Gholizadeh, 2013)

The suction suspension method cannot be used to all the situations. A gel liner is a good option when the condition of the residual limb is terrible. There is a pin extending at the end of the gel liner. The patient dons the gel liner by rolling it onto the residual limb and snapping it into the lock at the end of the socket. This pin-lock system allows the prosthesis well

suspended (Figure 2.4, Middle). The material for making gel liner are the silicone elastomer, silicone gels, and urethanes. These were good at shock absorption (Heim et al., 1997).

The seal-in liner utilizes a hypobaric sealing membrane around the liner to create a vacuum for suspension (Figure 2.4, Right). The benefits of using seal-in liner are to decrease the piston, translation, and rotation movements that occur inside the socket. The study found patients were more satisfied with the seal-in liner than other types. The polyethylene liner and locking liner were convenient for donning and doffing (Ali, 2012). The silicone liner as skin protection and cushioning intermediates between the socket and residual limb improved patients comfort and increased the function of the prosthesis and quality of patient's life (Kapp, 1999).

Most of the currently transfemoral prostheses are using suction or locking system for suspension. The comfortability of the prosthesis fitting is mostly dependent on the experienced clinic practitioners. Poor fitting results patients complaining about the loose suspension, pain on the residual limb and skin abrasion. To solve the prosthetic-related problems, the osseointegration had raised by Brånemark in the 1950s. It characterized as a stable fixation of titanium to bone tissue. This technique has been used in many clinic areas such as dental, facial prostheses, hearing aids, hand surgery, and orthopedics (Brånemark et al., 2001). The basic prototype is to insert a titanium fixture into the shaft of the femur while the patient completes amputation surgery (Figure 2.5). It requires six months' duration to help the fixture healing in place. During the healing process, the patient uses the traditional prosthesis to perform the daily activity. The further surgery is to screw a titanium rod into the fixture by penetrating the skin. It allows the prosthesis directly attaching to the residual limb.

Rehabilitation begins after six weeks' soft tissue healing and the whole accommodate to osseointegrated prosthesis around six months (Figure 2.6) (Smith et al., 2004).

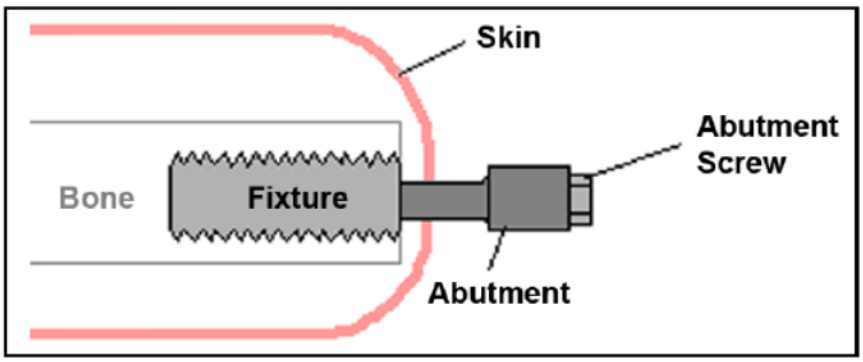

Figure 2. 5 Schematic view of implant system (Smith et al., 2004)

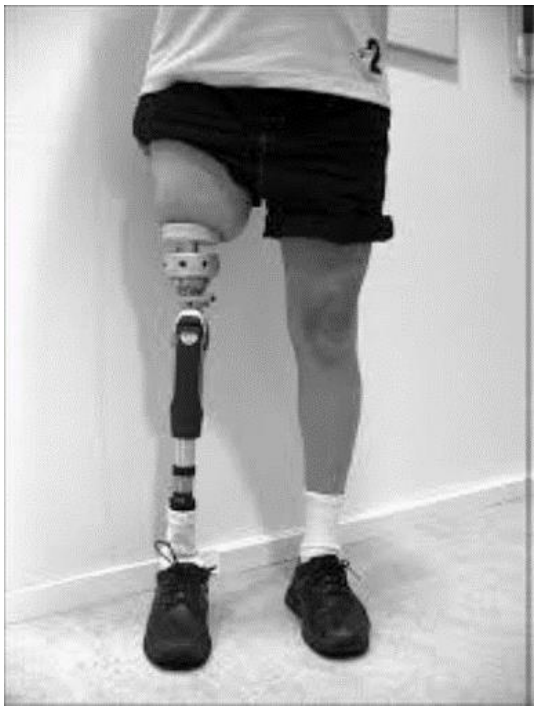

Figure 2. 6 Example of a patient using osseointegrated prostheses (Smith et al., 2004)

In a two years' follow-up study of 51 patients performing osseointegrated prosthesis, Hagberg et al. (2014) found that increased patient daily prosthetic use, and decreased energy

cost. Overall, the OI had the advantages of prosthetic control, improved stability, better fixation, maximum sitting comfort, the larger hip range of motion, quick donning and doffing (Hagberg et al., 2014). It is an alternative for transfemoral amputees who have experienced the traditional prosthetic socket and encountered problems such as skin ulceration, short stump length, soft tissue scarring. However, there are some criteria for the potential users to select the osseointegration:

1. The candidate tried the conventional prosthetic socket before;
2. The candidate is mature enough and has normal skeletal anatomy;
3. The candidate is not over 70-year old to tolerate the surgery;
4. The candidate's body mass is below 100kg;
5. The candidate has the good past medical history.

The complications for IP include: infection at the pin and skin surface interaction, loosen and bone infection (Brånemark et al., 2001; Sullivan et al., 2003). Therefore, the prosthetic socket will continue to be a practical provision to amputees using prostheses before the OI generally apply.

2.3 Development of CRS socket design

In the aforementioned traditional socket designs, the fit of the prosthetic socket is a matching process. A loose fit results in slippage and compromises stability; a tight fit increases stability but rises the interface pressure. Slippage is linked with the friction between the socket and the skin of the residual limb. Large friction offers the better suspension, but increase the shear force, which may induce tissue problems. The quality of fitting was much relying on the experience of the prosthetist (Schuch, 1999). Soft tissues are compressed when the amputee tries to apply residual force to operate the prosthesis. The control efficiency of the prosthesis is less effective due to relative motion induced by soft tissues compression between the femoral bone and the socket. Transfemoral CRS socket design is trying to enhance the socket control by pre-compressing the soft tissues along the shaft of the femoral bone. It utilizes the compression-release stabilization approach. There are four longitudinal depressions on the residual limb surface along the femoral bone to compress the residual limb, and four release areas adjacent allow tissues to displace (Figure 2.7, Left). With pre-compression, further motion of soft tissues is minimized. The momentum directly transferred through the thigh muscles to the socket without soft tissues' movement. There is no need for a high proximal socket profile because the thigh is better controlled, and more weight added to the femoral shaft. Socket suspension can be improved by compression/release structure (Figure 2.7, Right) (Alley et al., 2011; Resnik et al., 2014). A special casting apparatus is used to help achieving initial compression on the residual limb while taking a negative cast.

The CRS socket was trying to increase the stability control of prosthesis with tissue compression and relief physiologically through the appropriate locations on the residual limb

(Schofield et al., 2017). The compression accelerates the physiological changes to accommodate the residual limb atrophy and alterations of sensitivities, neuromas, etc. which the atrophy and changes accommodated (Cutler, 2017). The development of the CRS socket intents to achieve the function of osseointegration through the grasp the residual limb soft tissues.

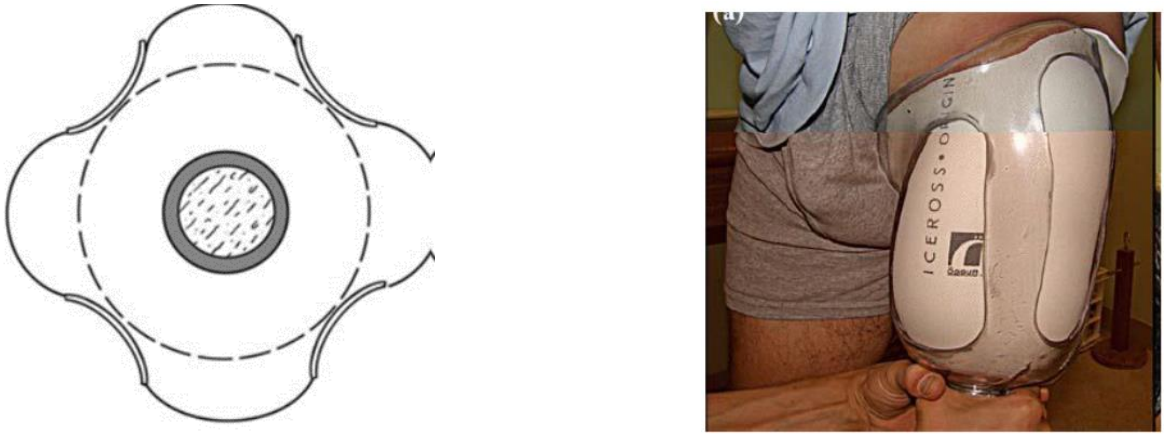

Figure 2. 7 Left, the compression/release diagram; Right, A CRS check socket fitting. (Alley et al., 2011)

2.4 Review of finite element study of the transfemoral prosthetic socket

Interfacial pressure is important in the design of prosthetic socket. The pressure sensor is a valuable tool for pressure prediction and has been used for about 60 years. The pressure measurement wass performed by placing the pressure sensor either between the skin and liner/socket or inserting within or through the socket and the liner (Mak et al., 2001). However, it cannot access the stress experienced by the residual limb and the condition inside the soft tissues. By dividing the complex structures into the small elements, the finite element method (FEM) was used to analysis the stress/strain state computationally and numerically.

The finite element method has been used in the prosthetic field to examine the prosthetic design, material properties, liners and stress distribution in recent decades (Prendergast, 1997; Reynolds & Lord, 1992; Zhang et al., 1998). The method allows the evaluation of stress, strain, and motion independent of the experimental approach and to analyze structure effects parametrically (Zhang & Mak, 1996). All these studies evaluated the single subject of the prosthetic socket fitting, and FE analysis is patient dependent and has to customize for the individual.

The finite element is a numerical method to solve the real problem by computational simulation. In FE, the big problem is discretized into a set of subdomains which combine the small elements and nodes (Figure 2.) (Cook, 1995). It was originally designed to predict stress for solid model in 2-D. A general procedure for a finite element analysis consists: pre-processing builds an FE model; solution utilizes the software to analysis, and post-processing shows the results. In 1998, Zhang et al. reviewed the finite element of study between 1987 and 1996 were the start of the FE model in the evaluation of interface stress in prosthetic socket.

The mathematical equation can be expressed as follow: $[K]\{u\} = \{F\}$

Where K is the property, F is the action, and u represents the unknown behavior of problems.

By rewriting the equation, the value of u can be calculated inversion of the matrix [K]:

$$\{U\} = [K]^{-1}\{F\}$$

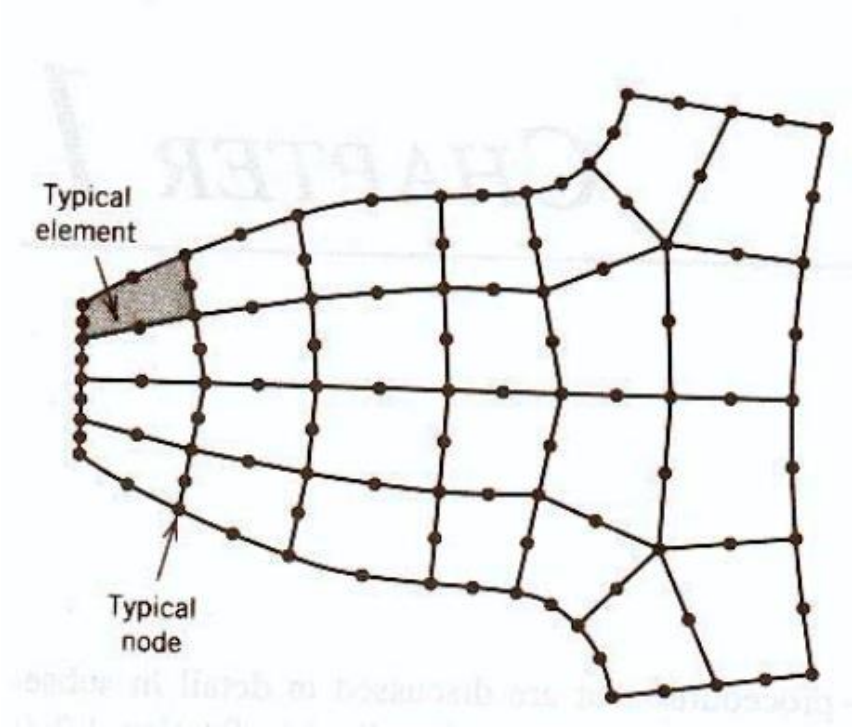

Figure 2. 8 A coarse-mesh, two-dimensional model of a gear tooth (Cook, 1995)

At the early stage of FE application in the study of prosthetic socket behavior, the FE models were mostly simple linear elastic for the soft tissue, homogeneous and isotropic for all the materials to reduce the computational cost. The socket was taken as the rigid object because it is harder than the soft tissue and difficult to access the material properties experimentally. The simulation of the socket rectification was achieved by nodes displacement on the socket or liner.

Previous studies mostly considered the soft tissue as the elastic springs. There is no slip at the skin/socket interface. The socket was taken as the rigid body. Zhang et al. (2013) conducted a 3D nonlinear model to consider the socket rectification and the slip/friction

condition between the skin and liner. It simulated the free limb state to fully donned into the rectified socket shape without additional external load.

The factors which influence the pressure distribution are liner stiffness, prosthetic rectification, the shape and relative bulk of soft tissue, the residual limb length, the stiffness/compliance of the residual limb soft tissues (Silver-Thorn, 1996). Brennan and Childress (1991) analyzed the ischial-gluteal bearing socket, partial IRC socket and total IRC socket.

The elastic modulus of the soft tissue can be obtained by either indention test or ultrasonic measurement to get the force-displacement relationship. Krouskop (1987) studied the AK socket using the FE model and measured the elastic modulus of soft tissue by using the ultrasonic method.

The finite element analysis in the prosthetic study was to describe the behavioral trend rather than stress values qualitatively. The effect of rectification process, residual limb-socket frictional force, and interfacial pressure were predicted by simplified 2D axisymmetric residual limb model. Homogeneity, isotropic and linear elastic were the assumption for the bone, soft tissues, and socket (Reynolds & Lord, 1992; Steege et al., 1987). Zhang & Roberts, (1970) conducted a 2D nonlinear finite element analysis of the below knee prosthetic socket interface pressure study. The geometry of the residual limb was obtained from an X-ray image, and entirely there were 1458 solid elements built in the FE model. It was the first time to study the slip effect of residual limb while considering the frictional force. The properties of limb tissues and liner were linear, isotropic, and local uniform. Young's modulus was

assigned differently with regions. The Young's modulus was calculated from the formula developed by Hayers et al. (1972).

$$E = p\,(1 - \upsilon^2) / 2kaw_0$$

Where E is Young's modulus, p the load applied by the indenter, υ the Poisson's ratio, a radius of the indenter, h the thickness of the measured layer (function of aspect-ratio (a/h) and υ), w_0 the depth of the indentation, and k the geometric and material-dependent factor.

Portnoy et al. (2007) developed a 2D FE model of the residual limb for real-time analysis and 3D model for calculating the internal stress and strains in the residual limb (Portnoy et al., 2008). The displacement of the residual limb with the hyperelastic material property was simulated for donning the transfemoral prosthetic socket. However, the overclosure did not consider in that research. Ramírez & Vélez (2012) studied the effect of the boundary conditions between bone and soft tissue using FE model for a transfemoral amputee found that the magnitude and distribution of stress and strains significantly influenced by the friction between bone and soft tissue. Zhang et al. (2013) applied hyperelastic material properties for the soft tissue to simulate the friction between the skin and the transfemoral socket. It also studied the influences of load transfer between limb and socket by adding vertical loads to the bottom of the socket surface to simulate the foot flat, mid-stance, and heel offloading conditions.

The nonlinear elastic material properties were implemented using the Mooney-Rivlin model (1940) with a polynomial strain energy function of the form

$$U = C_{10} (I_1 - 3) + C_{11} (I_1 - 3) (I2 - 3) + (J - 1)^2/D_1$$

Where U is the strain energy potential, I_1, I_2 the first and second deviatoric strain invariants, J_1 the elastic volume ratio, and C_{10}, C_{11}, and D_1 the material parameters. If D_1 is zero, the material is fully incompressible.

The accuracy of the FE simulation depends on the modeling of material properties, geometric data, loading characteristics, boundary and interfacial conditions. Other factors to determine the socket fitting are the slippage of the socket and the interfacial connecting stiffness – the relative movement between the bone and the socket.

The summary of finite element analysis of prosthetic shows in Table 2.1. The studies on the transfemoral (TF) prosthetic sockets finite element analysis were less than transtibial (TT) sockets. The majority of the previous FE researchers evaluated the single case and static condition firstly.

Table 2. 1 Characteristics of residual limb interface mechanic model

Reference	Element Type	Material Properties						Level
		Tissues		Bone		Socket		
		E (kPa)	υ	E(MPa)	υ	E(MPa)	υ	
(M. Zhang et al., 1995)	-	260/160, 200	0.49	10	0.49	Fixed boundary	-	TT
(Lee et al., 2004)	Automated contact, both friction/slipping	200	0.49	10 GPa	0.3	1500	0.3	TT
(Sanders & Daly, 1993)	Linear, homogeneous, isotropic	5.2-skin 131-muscle	0.49	-	-	1.8 pelite	0.39	TT
(Faustini et al., 2006)	Linear elastic, homogeneous, isotropic	200	-	15GPa	0.3	1.6Gpa 380kPa-	0.39	TT
(M. Zhang & Mak, 1996)	Linear, isotropic, homogeneous	150	0.3	15GPa	0.3	15GPa	0.3	TF
(Lee et al., 2004)	Linear, isotropic, homogeneous	200	0.45	-	-	1500	0.3	TT
(Zachariah & Sanders, 2000)	Linear, isotropic, homogeneous,	965	0.45	69000 for shank	0.3	1000	0.35	TT
(Silver-Thorn, 1996)	-	60	0.45	-	-	1000	0.3	TT
(M. Zhang & Roberts, 2000)	Isotropic, linearly elastic	200	0.49	15GPa	0.3	380GPa	0.3	TT
(Jia et al., 2005)	Linear, isotropic, homogeneous	200	0.49	10GPs	0.3	380K-P	0.39	TT
(Lin et al., 2004)	Linear, isotropic, homogeneous	-	-	15500	0.28	rigid	-	TT
(Commean et al., 1997)	-	60	0.49	15500	0.28	14000	0.13	TF
(Lacroix & Patiño, 2011)	Hyperplastic soft tissues	-	-	15G	0.3	1.5G	0.3	TF
(L. Zhang et al., 2013)	Hyperplastic soft tissues	C	0.459	15000	0.3	15000	0.3	TF

2.5 Pressure measurement of prosthetic socket-residual limb interface

The measurement of pressure was mostly performed by inserting the pressure sensor between the limb surface and inner wall of the prosthetic socket. Based on the principle, the sensor is classified as strain gauges, piezoresistive, capacitive, optical sensors. The classification and characteristics are shown in Table 2.2.

Table 2. 2 The classification and characteristics of pressure sensors extracted from (Al-Fakih, 2016)

Sensor characrestic	**Sensor types**	**Disadvantages**	**Disadvantages**	**Parameters**
Transducers mounted on socket wall	Strain gauge	high accuracy, and sensitivity	Socket with holes, Bulk, lower spatial resolution,	Strain, normal and shear stresses, forces
Transduces inserted in socket	Piezoresistive	No modification of	Non-linearity, drift, hysteresis, temperature sensitivity, cannot measure shear stresses	Direct contact pressures
	Capacitive	Flexibility, operational accuracy + 20%	Rigid substrates do not fit limb geometry, limited use in socket	Fore, pressures, displacement
	Optical-based transducer	Accuracy, sensitivity	Susceptible to EMIs, bulky	Normal and shear stresses, Displacement
	F-Socket	Pressure all over the residual limb, high spatial resolution	Hysteresis, drift, crease, fail, unable to measure shear stresses	Normal pressure
Transducer embedded in socket wall	Fiber Bragg Grating (FBG) sensor	High sensitivity, durability, immunity to electromagnetic interference (EMI), multiplex ability, resistant to harsh environments,	Full operation might be hampered due to any damage to the optical fiber	Strains, forces, Normal and shear stresses, vibration, temperature,

The selection of the sensor for the lower limb pressure measurement depends on the purpose and interface of the experimental design. However, they share the common characteristics (Partsch, 2006).

1. Thin and flexible, be able to measure on the flat surfaces;
2. The sensitivity can be adjusted and accommodate on different curvatures;
3. It is hardly affected while the skin condition changes during measurement;
4. Continuously pressure detection;
5. Easy calibration;
6. The sensors measure the pressure at different location same time.

Rincoe socket fitting system, Tekscan F-socket pressure system (Tekscan Inc., South Boston, MA, USA) and Novel Pliance 16P system are the pressure measurement systems available in the market. F-socket is a paper-thin with high resolution. It is placed within the socket to measure the residual limb interface pressure. It can be trimmed into freely floating fingers to meet the curvature of the socket interface. The sensor is 0.178mm thick and consists of 96 sensels (Maurer et al., 2003)

The Strain gauge-based transducer has the high accuracy and sensitivity, but the socket needs to be modified to mount the SG pressure transduces. This makes it difficult to achieve when the patient did not want to change their socket. The F-scan sensor cannot measure the shear stress. The Fiber Bragg Grating (FBG) gains the most advantage on the strain, shear, and normal stress measurement. However, the optical fiber is easy to damage.

The FBG uses the optical fiber to reflect wavelengths of light in a type of distributed Bragg reflector. It has been widely used in the aeronautic, automotive industry, undersea oil exploration and recently utilized in the biomechanical evaluation of prosthetics and orthotics (Al-Fakih et al., 2012; Kanellos et al., 2011). Al-Fakih et al., (2013) first full-scale implemented the stress and pressure simultaneously on a transtibial amputee. However, this has not been commercialized yet in the P&O field.

2.6 Coefficient of friction

Friction is an important factor to prevent the socket from slipping under the gravity and momentum during the swing phase of the gait. The slippage of the socket is an indication of socket tightness. An absolute non-slippage of the socket with the residual is not possible. The socket control and stability can be improved if the socket is tight enough, vice vise it would cause instability and even lose out the residual limb during the swing phase. The patient feels discomfort like buffer inserted between the skin and socket. There is a lot of researches to study the effect of shear force and slippage induced by the friction between the skin and different materials. In 1998, Sanders and colleagues studied the human skin coefficient of friction with eight interface materials. The range of coefficient of friction was found to be 0.48 to 0.89. Zhang and Mak (1999) reported an average coefficient of friction 0.46 in vivo human skin with five materials. The friction helps to assist the prosthetic suspension but also cause skin breakdown due to shear force. Zhang et al. (1996) found that the friction was proportional to the shear stress but disproportional to the normal stresses. Their studies suggested an appropriate coefficient of friction was required to support the loads and prevent the slippage and shear stress-induced skin problem.

CHAPTER 3 DEVELOPMENT OF THE DESIGN FEATURES OF CRS SOCKET AND FINITE ELEMENT MODELING PROCESS

3.1 Pilot study 1- initial compression/release stabilized (CRS) socket design

There are two ways to get the geometry of socket: directly scanning the residual limb and modify the image using the software to build the socket shape or using the plaster to take the negative impression of the residual limb. The modification and design of socket model are performed on the plaster filled negative impression.

However, to build the FE model for the CRS socket, the geometry of the socket has to be obtained from the scanning of the socket or the residual limb. It was difficult to scan the transfemoral residual limb because the residual limb had to keep in the adduction during the scanning. This position prevents the access of medial side surface of the limb. In order to get accurate residual limb geometry, a cast was taken for the amputee in this study. The scanning was performed for the positive cast of the residual limb.

A casting apparatus was developed to assist the CRS casting. Five compression depth CRS socket was evaluated to find the appropriate baseline for FE modeling. The flow of this study shows in Figure 3.1

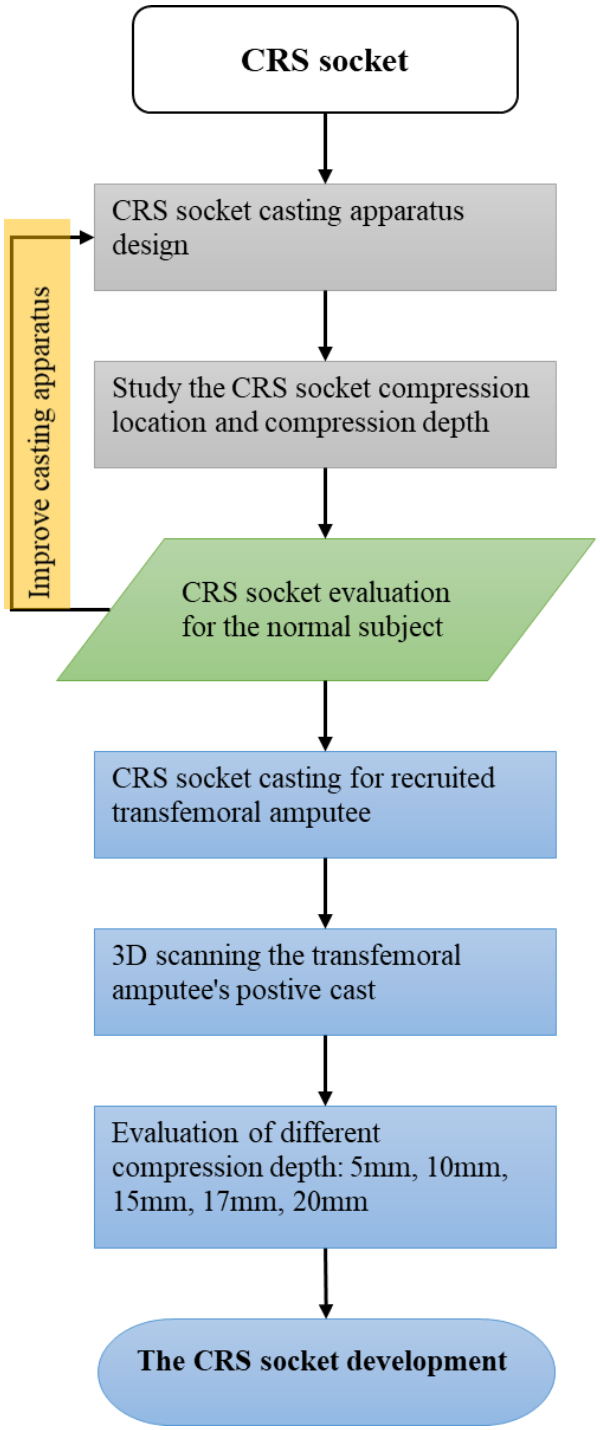

Figure 3.1 Flowchart of CRS socket development

3.1.1 Development of a casting apparatus

A casting apparatus was developed for the casting of the residual limb to achieve the compression/release objective. Figure 3.2 is the casting apparatus developed in this study. The primary components of the apparatus are quick release grips connected with aluminum bars which for the compression purpose. It is connected to a casting stand (Ottobock, German) to allow adjustment of the height. The aluminum formed framework supports the grips and a stand to hold the frame, which enables it to adjust the height.

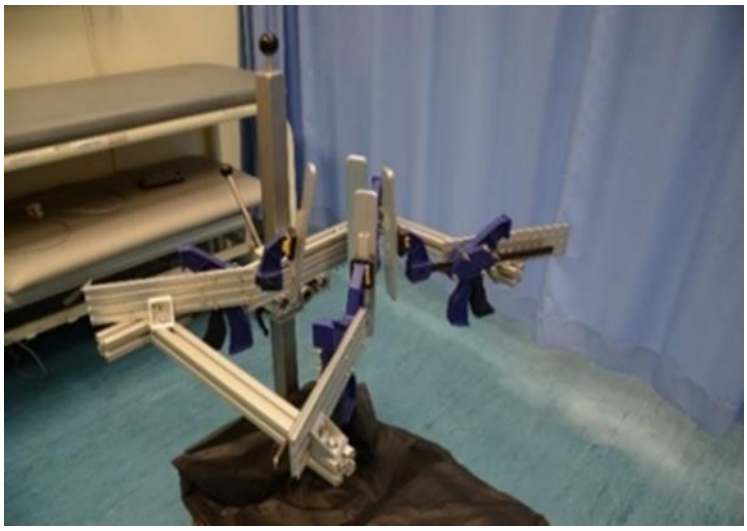

Figure 3. 2 A prototype of casting apparatus

According to Newton's law, the resultant force is zero, and there is no shear force and rotational moment if the force and counter force is same magnitude but opposite direction aligned within the same line. Therefore, the shape of the thigh is assumed to be a cylinder in this study and divided the cross-section of thigh into four equal partitions by the middle sagittal and coronal plane.

The compression directions were initially set at the middle of (45 degrees) each region: the anterior-lateral (A-L), anterior-medial (A-M), posterior-lateral (P-L) and posterior-medial (P-M). The compression force applied on anterior-lateral and posterior-medial, anterior-medial and posterior-lateral were acted as force and counter-force along a straight line with the same magnitude and opposite directions. This allocation minimized the shear force and rotational movement according to Newton's law and the Pythagorean theorem.

The diagram shows the compression forces acted on the 45-degree and 30-degree direction and its x and y composite (Figure 3.3). F_{AM} F_{AL} F_{PM} F_{PL}

The law of composition of force implies:

$F=F_x + F_y$ $F_{45d}=F_{45x} + F_{45y}$ $F_{30d}=F_{30x} + F_{30y}$

According to Pythagorean Theorem

$F_{45x} = F_{45y} = \frac{\sqrt{2}}{2}F_{45d}$ $F_{30x} = \sin 30 F_{30d} = \frac{1}{2} F_{30d}$

$F_{30y} = \cos 30 F_{30d} = \frac{\sqrt{3}}{2} F_{30d}$

The force F_{45x} and F_{45y} are the same magnitudes from the above equation. The CRS compression location was assigned in the 45 degrees to reduce the rotational movement.

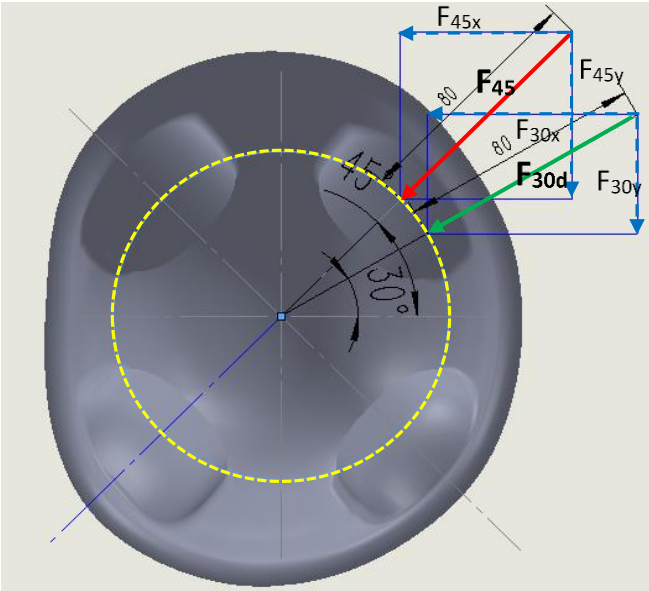

Figure 3. 3 The direction of compression force. The red arrow represents the force exerted on the 45 degrees, F_{45d}. The green arrow represents the force exerted on the 30 degrees, F_{30d}.

From the literature, the circumference of midthigh was from the 467±40mm to 515±41mm for Whites and Asian males and females (Table 3.1). The mean was 492±41.5mm. The width of the compression bar was calculated by divided this mean value with 8. Because there were four compressions with adjacent four release areas in CRS socket design, the width of compression area was approximate same with the adjacent opening. The measurement was taken from the ischial tuberosity to the lateral femoral condylar with a 50mm interval. The width of compression bar formula shows below:

$Width_{A\text{-}L}=Width_{A\text{-}M}=Width_{P\text{-}L}$-l=$Width_{P\text{-}M}$=492mm (midthigh circumference)/8=60mm

Table 3. 1 Comparisons of circumferences at six sites between Whites and Asians' (Wang et al., 1994)

	Males		Females	
Upper chest	Whites (n=187)	Asians (n=110)	Whites (n=258)	Asians (n=132)
		mm		
Arm	310±34	297±33[2]	273±32	269±29
Upper chest	1007±67	946±60[3]	861±55	838±55[3]
Chest	993±73	920±66[3]	890±80	854±70[3]
Waist	878±89	831±84[3]	734±85	731±84
Iliac crest	937±83	897±72[3]	919±85	887±73[3]
Thigh	515±41	492±41[3]	494±44	467±40[3]

[1] $\bar{x}$ ± SD

[2,3] Singificantly different from whites of same sex: 2 P = 0.0014. 3 P = 0.0001.

3.1.2 Testing casting apparatus on a normal subject

A 38-year old healthy subject was cruited in this study to improve the casting apparatus. He was instructed to put his right leg inside the casting apparatus with the hand supporting on the casting stand for the safety issue. The compression bars were set at the level of thigh. The compression bar was set in a straight line with the opposite one to reduce rotation of limb under compression. The prosthetist gradually adjusted the compression bars from just in touch with the residual limb surface to fully compressed position several times to test the subject's tissue tolerance. A notification was marked on each compression bar to record when the subject verbally reported that he felt the compression was strong enough to secure the thigh but did not induce the pain or discomfort. The prosthetist started to measure the limb circumference from ischial level and 50mm downward increment for each. The measurement was taken under two conditions: ① the soft tissue was relaxed; ② the soft tissue was in the

fully compressed position, which means the measurement tap was tensioned to no further change around the thigh tissue and the subject did not report discomfort.

The procedure of the casting had been tested several times before the formal casting started. The subject was given detail instructions to cooperate. The plaster bandages were used to get the negative impression of the subject's right thigh outside the compression area. There were four layers of plaster bandage wrapping on the thigh based on the prosthetist's experience. When the wrapping finished, the subject quickly put his right limb inside the casting apparatus.

Four rotatable pressure pads were compressed onto the outer surface of the plaster wrapped limb to form the compression on the soft tissue of the thigh (Figure 3.4). The prosthetist moved the grips to the position previous marked and adjusted slightly according to the subject's response. The positive cast of right limb was made from filling the plaster to the negative impression. Rectification of the positive model was done by a qualified prosthetist.

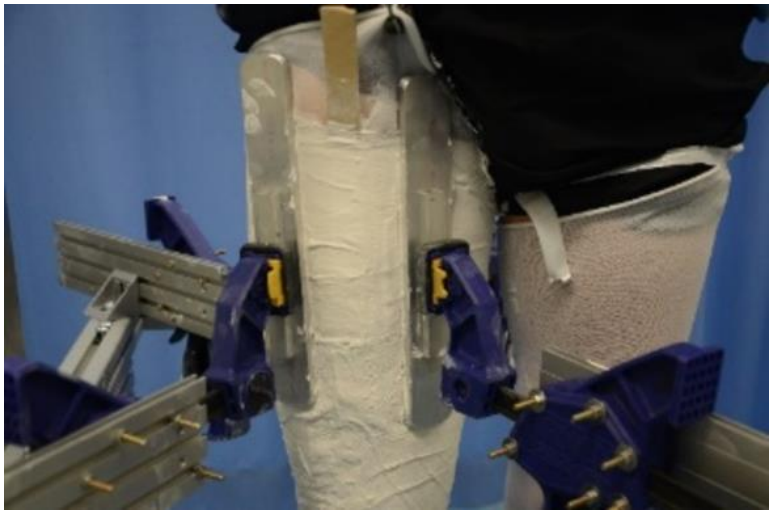

Figure 3. 4 Negative impression of CRS socket

3.1.3 Check socket for the normal subject

A socket was made for the normal subject using 15mm thermolyn plastic. The posterior side of the socket was opened for better donning and doffing. The subject donned the socket with the knee flexed 90 degrees. There were three straps on the opening to control the tightness of socket. The compression forces were affected by the adjustment of straps. The subject walked along a 10-meter walkway and the personal feedback collected for the improvement of the socket design. Figure 3. shows the process of CRS socket design from casting to fitting.

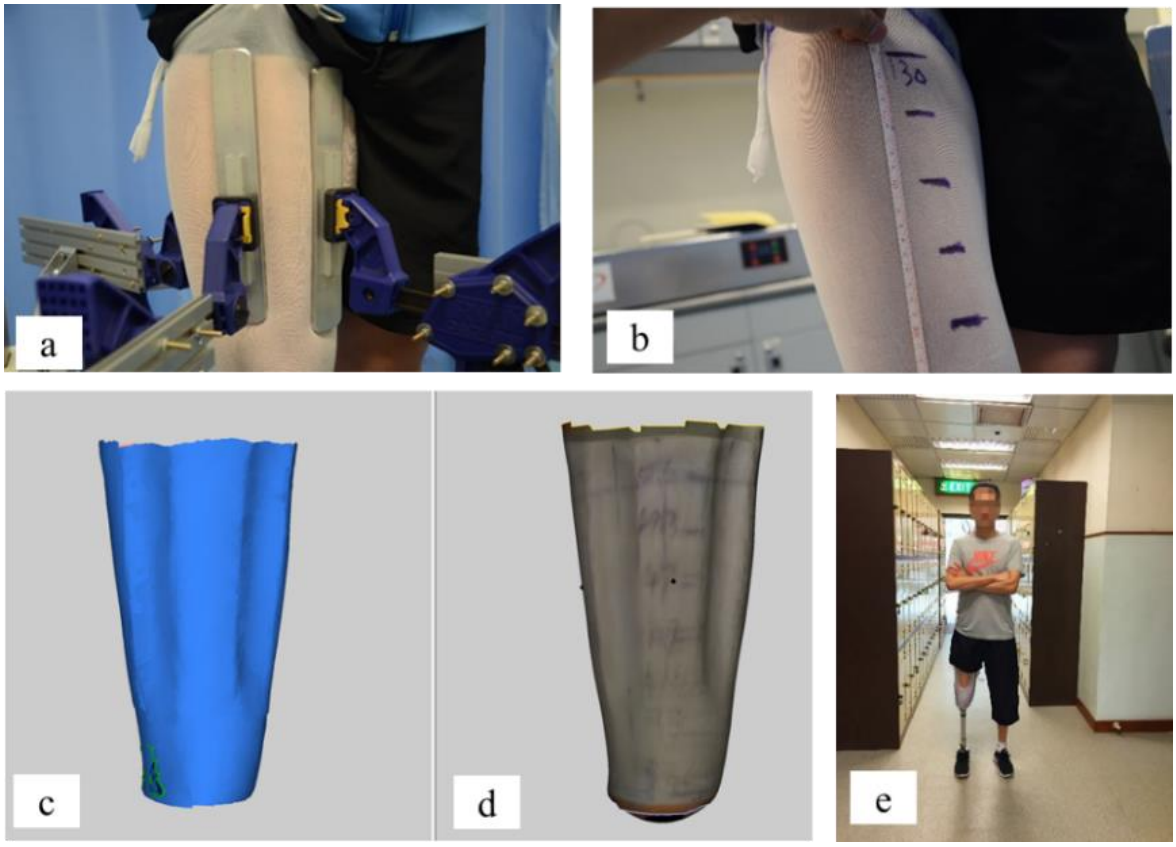

Figure 3. 5 The process of CRS socket design from Casting to fitting. a, the compression orientation test before the casting; b, the measurement started from ischial tuberosity level; c, the scanned 3D socket for normal subject d, the positive cast scanned; e, the normal subject wore the CRS prosthesis with his right knee flexed.

3.2 Development of CRS socket features with a transfemoral amputee

The trial study of CRS socket on the normal subject guided the casting and modification of CRS socket. However, there were some limitations of the casting apparatus:

- It was difficult to adjust the active compression force and counter-force in line;
- The compression bars would rotate once the compression force was large;
- The desired compression value was difficult to achieve while the bandages applied.

To build an FE model for the recruited transfemoral amputee, it had to get a reasonable CRS socket structure. Five different compression values (5mm, 10mm, 15mm, 17.5mm, and 20mm) were applied to construct the CRS socket for the transfemoral amputee. One negative impression of an amputee's residual limb was taken by a prosthetist. The positive model was obtained by filling the plaster into the negative cast. After smoothing, the positive cast was scanned by using the 3D scanner (Vorum Spectra^{TM}, Canada). The geometry of the subject's residual limb and each positive cast of residual limb model were scanned by the 3D scanner as well. The depth of the compression was made by using the Catfit^{TM} CAD software (Vorum, Canada) to make five sockets. The CAD designed five CRS sockets were sent to Prince of Wales Hospital where the computer-aided manufacturer machine located. The five positive foam models of CRS socket were created by CAM milling machine. Each CRS socket was thermoformed by 5mm thick high temperature polypropylene (Figure 3. 6).

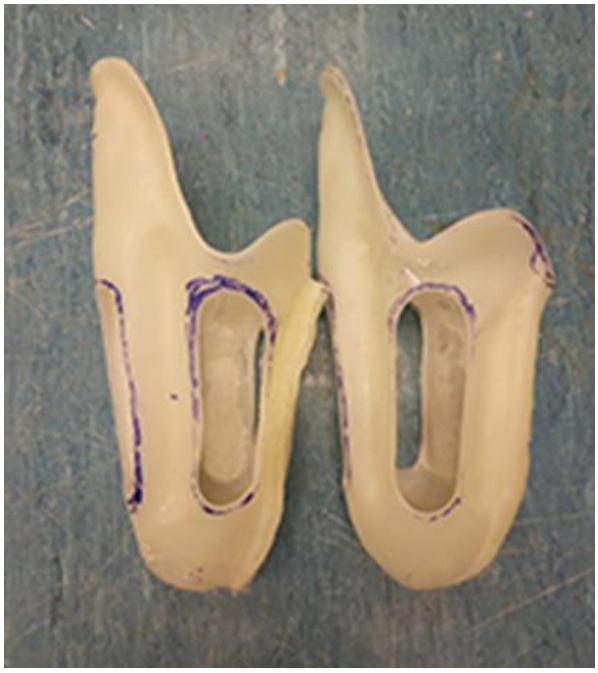

Figure 3. 6 The CRS socket. left, 10mm compression; right 15mm compression

3.2.1 Subjective response

The pressure measurement of the prosthetic socket can give us objective result of socket design. However, subjective feedback is also important which unpleasant feelings of wearing prosthesis would be torture for the patient. The using of questionnaire evaluation is a way to collect the subjects' perceptions. Prosthesis Evaluation Questionnaire (PEQ) is one of prosthetic outcome measurement instrument which is widely used in the research and clinic (Boone & Coleman, 2006). It consists of nine functional domain scales covering 54 questions in the major area related to amputations. Each domain scale is independent with others and can be used separately. The Cronbach α coefficients for the subscales of PEQ is ranging from 0.73 to 0.89, which shows a good reliability (Condie et al., 2006; Gauthier-Gagnon & Grisé,

1994; Legro et al., 1998). Nevertheless, the visual analogue scoring (VAS) of PEQ is difficult to interpret, and the ipsative feature of VAS makes it problematic in the repeated measurement designs (Wewers & Lowe, 1990). The questions used in this study were modified from the PEQ. The five scales rating was employed instead of VAS to collect the answer. The questionnaire was developed to collect the personal feelings about the CRS socket while the patient was donning the prosthesis and when the full body weight (800 Newtown) added on. The questions covered the satisfaction of patient standing and sitting comfort of CRS socket, pain feelings during donning and doffing of CRS socket, the overall feedback of socket and open comments that he wants to make. Five scales for individual questions was set from 1 to 5 with 1 representing the most terrible situation and 5 feeling excellent. The score 3 meant not too bad or good (Appendix II). The simplified PEQ has not been validated. It should be validated before used for further study.

The subject responded that there was no pain (score 3) for the CRS socket with 5mm, 10mm and 15mm compression depth while donning, doffing, full-weight bearing and sitting. It was painful while using 17.5mm and 20mm compression socket. The pain mostly concentrated at the edge of the opening where the soft tissues protruded out of socket due to excessive compression at the compression areas. The skin color at these regions turned red after he took off the socket. Regarding the comfortability, there was no difference between 5mm, 10mm, and the patient's own IRC socket. It revealed the 15mm compression was the most comfort (score, 4) and no pain (score, 5) compared with other values. Therefore, the 15mm was selected on the design of the CRS socket for the subject. The patient's response to the comfort and pain after fitting the CRS socket shows in Figure 3. 7.

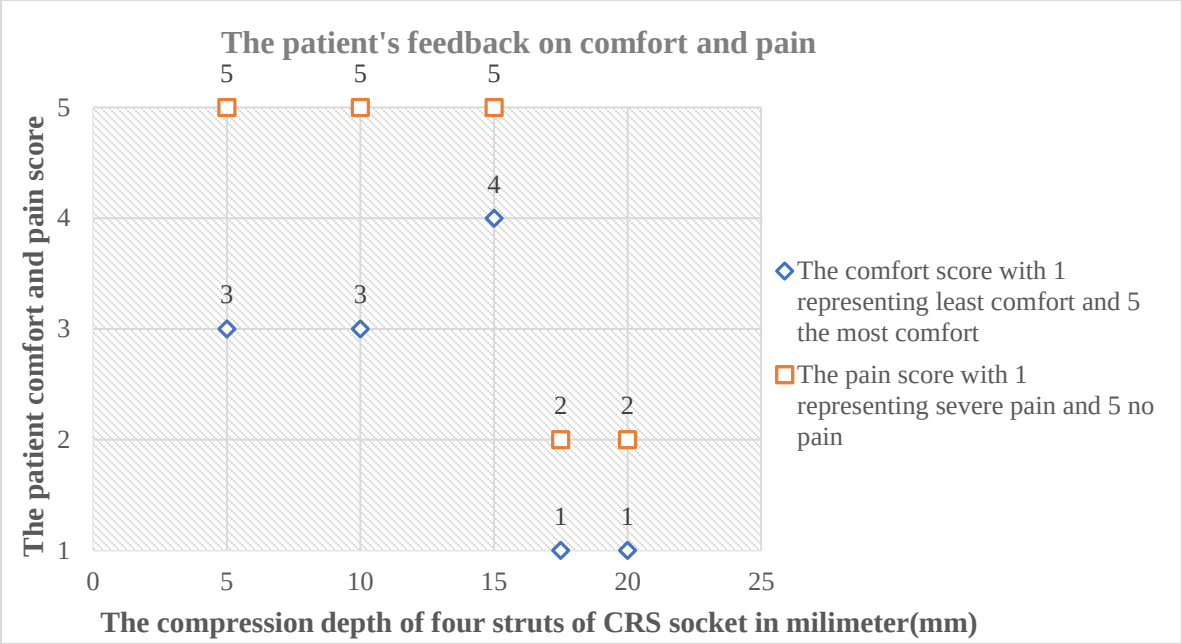

Figure 3. 7 The patient's comfort and pain score on CRS socket

3.3 Pilot study 2 – develop a finite element modelling process

To build a finite element model, the patient's residual limb geometry and the CRS socket were the essential elements. In previous studies for evaluation of conventional IRC or Quad socket, the socket was designed and fitted by the prosthetist. Because the compression/release stabilized socket design is relatively new, and there is no much research work on the CRS study. The instructions on how to design a CRS socket has to be initiated, as it is the key part of the evaluation. The development of finite element model is a time-consuming process, and it takes time for patient to prepare the MR scanning. To reduce the error during the FE modeling and experimental validation, a pilot study was performed for a transfemoral amputee (44-year old female's CT image from our research team) to familiar and understanding the desired methodology before the actual experiment start. It was designed to find a method to build the CRS socket and enhance the finite element modeling proficiency. The aims were:

1. To quantify the CRS socket design through the healthy subject and recruit transfemoral amputee subject;
2. To 3D reconstruct and segment from a female transfemoral amputee CT image;
3. To develop an FE model for the female subject;
4. To design the CRS socket based on the subject's 3D reconstruction image;
5. To study the interfacial stress and strain between the CRS socket and residual limb by finite element method.

The flow chart for this preliminary study shows in Figure 3.8.

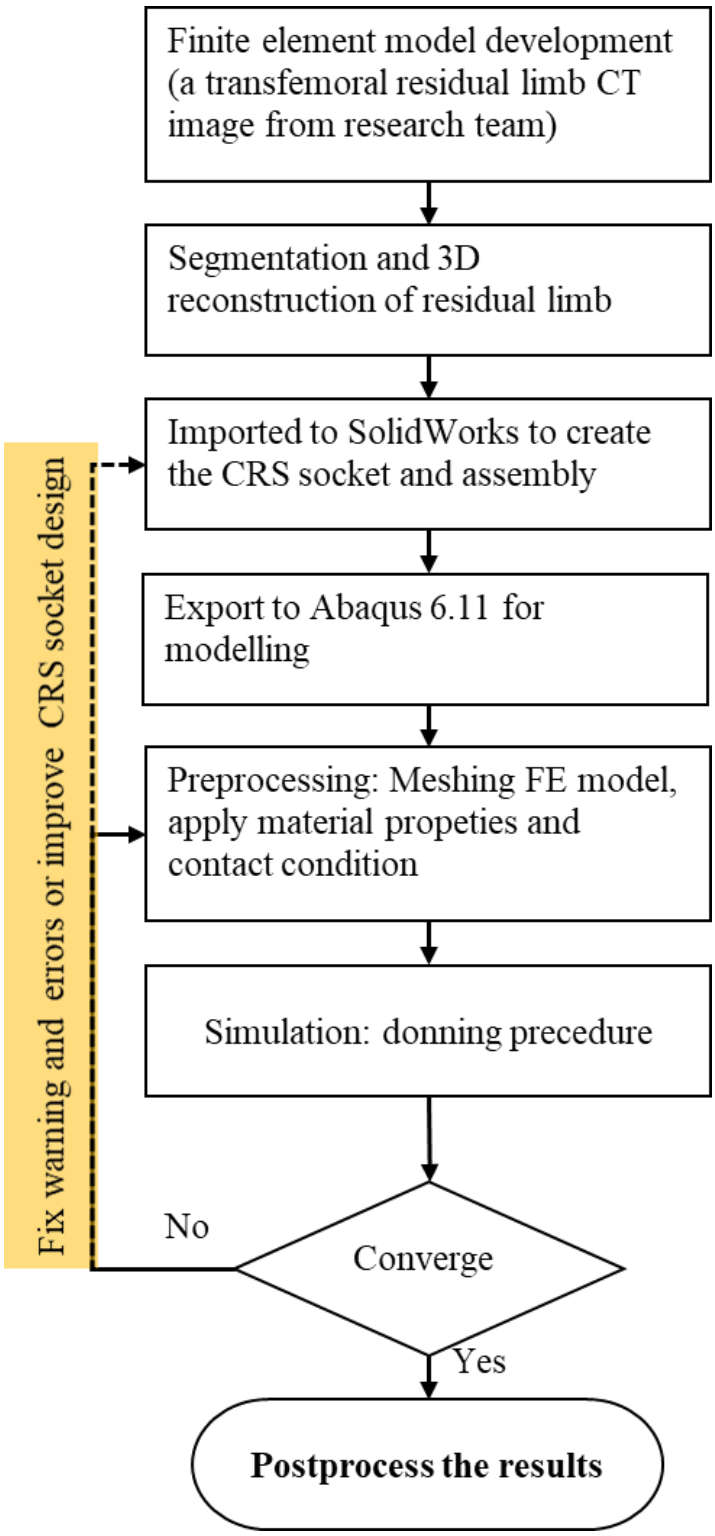

Figure 3.8 Flowchart of initial FE modeling

3.3.1 Segmentation and 3D reconstruction

In the FE analysis, several softwares were utilized sequentially to achieve the goal. These included Mimics (Materialise, Belgium), Geomagic Studio (v 13, Raindrop Geomagic Inc., USA), SolidWorks (SolidWorks Corporation, MA, USA) and Abaqus (Dassault Systèmes, RI, USA). Mimics performs the visualization and segmentation functions of 2D CT image and constructs the 3D objects of the image. It generates the STL file for fast prototype like 3D printing. The first step was the 3D construction and segmentation of the 2D CT image.

CT DICOM file was imported into mimics through new project wizard. It had to check the detailed information such as pixels and orientation showing on the tags during the importing process (Figure 3.9).

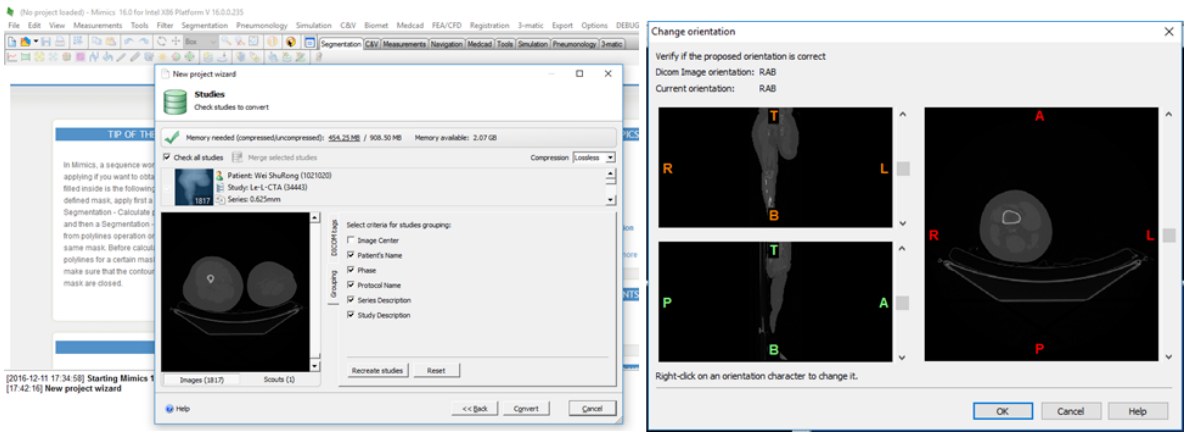

Figure 3.9 DICOM file importing process

A new mask was created to segment the bone and tissues from the 3D image. The mask was a group of pixels representing the 2D images of original object but independent from original images. The data stored in the mask is either 0 or 1. Under the mask, the thresholding

interprets the image with the gray value from -1000 to 3000. The normal range for bone is between 100 and 300, and should be adjusted and selected based on the output 3D image quality. The gray value affects the quality of the object. Most of the time there are many holes in the structure. Appropriate gray value is essential for maintaining the optimal quality and make it easy to segment. A lower gray value shows more details but increases the noise. A high gray value reduces the noise but increases the information missing. Therefore, the gray value was carefully chosen to show the rebuilt 3D object. After several attempts, the minimal gray value selected in this study for bone was 150. This value allowed us to separate the bone from the regional tissues by using region growing function. The holes were filled by manually adjusting the 2D images at three plans slice by slice using the editing tool. The constructed 3D object was processed by the smooth and wrap function. The 3D construction of residual limb was achieved similarly (Figure 3.10).

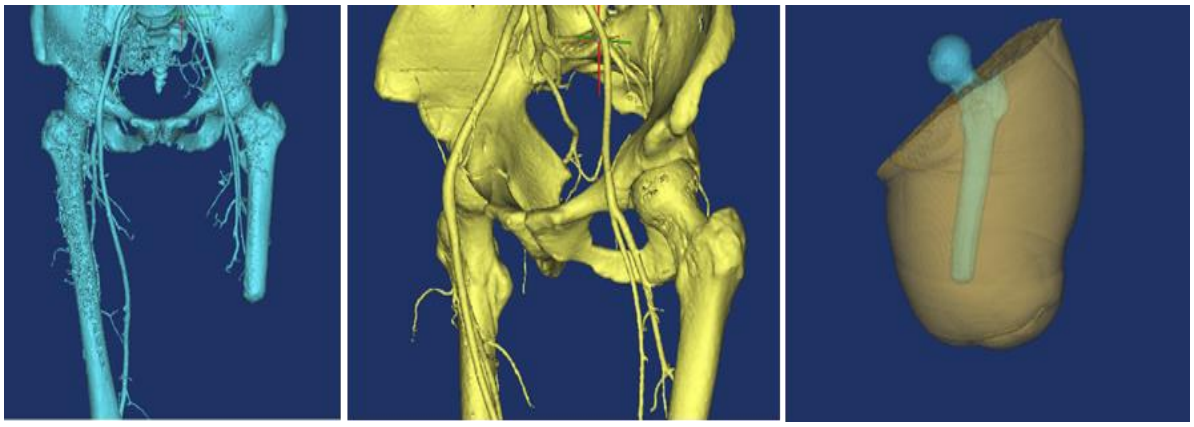

Figure 3.10 The 3D reconstruction of Bone and soft tissue

3.3.2 CRS socket design based on the 3D model of the residual limb

There are two ways to get the geometry of socket: (1) taking a negative impression and subsequently rectification of positive model, and (2) directly scanning the residual limb and modify the image using computer software. The modification and design of socket model can be performed on the plaster filled negative impression. During the scanning, the residual limb needs to maintain a neutral hip position. However, the scanning of the medial side of the residual limb was difficult if the hip joint of the amputated side was not abducted. In this study, a negative impression of residual limb was taken first, and then the rectified positive model was scanned for the socket fabrication.

The geometry of soft tissue was obtained by removing the femur bone from the residual limb. The surface model of bone and soft tissue was exported to reverse engineering software Geomagic Studio (v 13, Raindrop Geomagic Inc., USA) to convert into a NURBS model (Taddei et al., 2007).

The construction of CRS socket and assembly of soft tissue and socket were performed in the software SolidWorks (SolidWorks Corporation, MA, USA). Four compression areas were created at the anterior-lateral and posterior-medial, anterior-medial and posterior lateral position, which were 45 degrees within the middle sagittal and middle frontal planes. The socket thickness was made by the 4mm thicken around the modified residual limb surface (Figure 3.11).

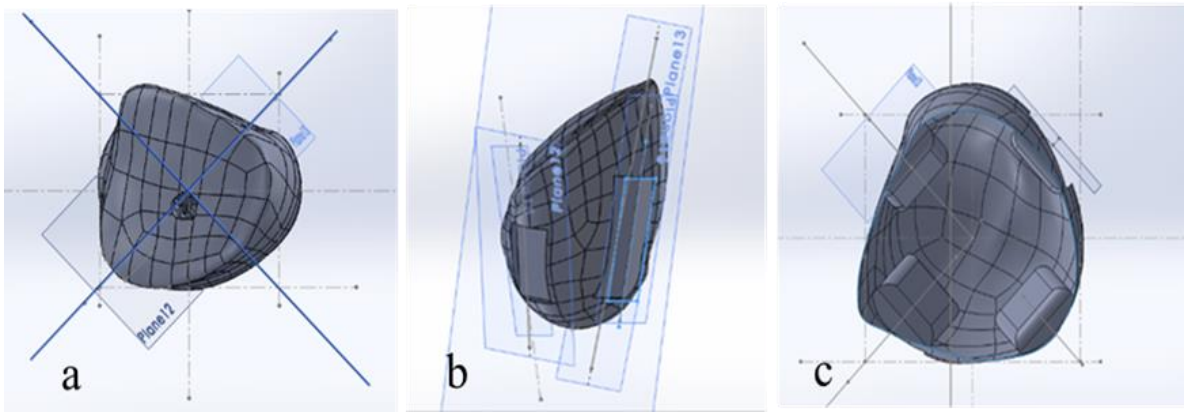

Figure 3.11 The 3D residual limb modification and CRS socket design in SolidWorks a, the top plane view of soft tissue model; b, modify the soft tissue by using the extruded cut function at desired compression areas; c, prosthetic socket developed by offset 4mm of modified soft tissue

3.3.3 Material models and boundary conditions

The mechanical properties of the bone, soft tissue and socket were assumed to be linear elastic, isotropic and homogeneous. The Young's modulus of bone and socket was set 15000 MPa and Poisson' ratio 0.3 (Vélez Zea, 2015). The Young's modulus of soft tissue was modeled with value 0.2 MPa and 0.45 for Poisson's ratio (Table 3.2) (Lee, 2004).

Table 3.2 Material properties for bone, socket and residual limb

	Young's modulus (MPa)	Poisson's ratio
Bone	15000	0.3
Socket	1500	0.3
Soft tissue	0.2	0.45

3.3.4 Contact conditions

The contact condition for socket and soft tissue was set a surface-to-surface contact where the more rigid surface of socket defined as master surface and slave surface for residual limb. Because of the large overlapping and sliding, the coefficient of friction between the two contact surfaces was chosen as 0.3, which was the minimum value from literature in the amputee subject study. The bone and the residual limb were bonded together with a tie contact which prevented relative slave nodes sliding with the master surface. The prosthetic socket was initially assigned with the residual limb with a vertical displacement vector to simulate the pre-stress condition while donning the prosthesis (Figure 3.12, 3.13) (Lacroix & Patiño, 2011). The value of displacement was calculated in the SolidWorks. In the SolidWorks, the right plane and frontal plane of the residual limb and socket were all mated coincident. The socket was allowed to move in the Z direction and initially in touch with the residual limb. The distance measured from the top plane of the residual limb to the CRS socket was the displacement for residual limb from in touch with socket fully donned position. This value was found to be 168mm.

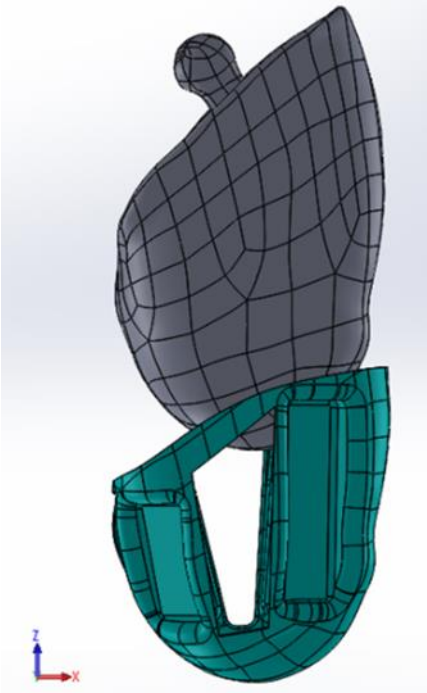

Figure 3.12 The assembly of residual limb and socket model

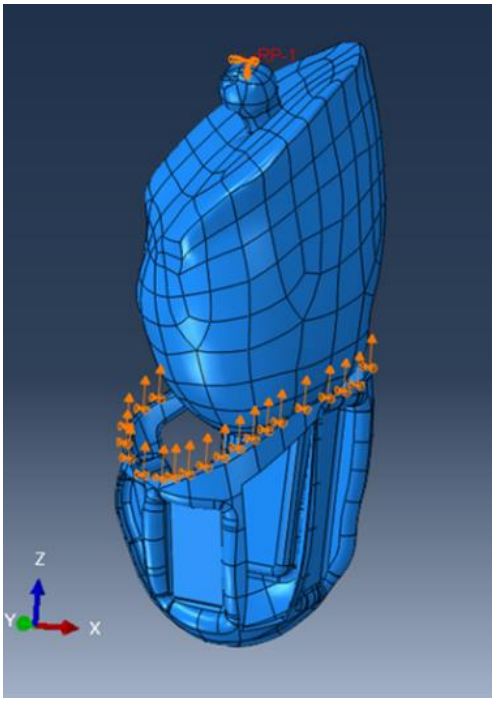

Figure 3.13 The vertical vector applied at the upper brim of the socket in Abaqus

The mesh type for the bone, soft tissue and socket were tetrahedral meshes, which were preferred for the complex geometries than hexahedral meshes in the prosthetic study. While using the ten node-quadratic tetrahedron (C3D10), the number of nodes was ten times than four nodes tetrahedron (C3D4). Therefore, the C3D4 node type was used in this study to reduce computational time. The mesh element size was set 4mm for the bone, soft tissue and socket. The detailed mesh elements show in Table3.3.

Table 3.3The mesh elements detail

Subject	Material	Number of nodes	Number of elements	Element size
Amputee (CT image)	Bone	2788	12740	6mm
	Socket	5635	18012	10mm
	Residual limb	19184	102928	7mm
	Total	27607	133680	N/A

3.3.5 The results of FE simulation

Stress and displacement in bone, soft tissue, and socket the were predicted. The maximum stress and displacement were observed on the femur bone. This was probably due to the force directly loaded on the femur head. The pilot study only focused on the interaction between the inner socket and residual limb. The FE simulation of amputee's model had aborted around 40% percent of the processing. The result of normal stress and displacement shows in Figure 3.14 and 3.15 respectively. The peak pressure observed 189 kPa in the anterior-lateral compression area. The maximum displacement was 34.9mm in the same region (Figure 3.16). It cannot converge after trying of mesh refining and adjusting the parameters. It was likely that the protuberance of the upper part of compression struts were too sharp to move the socket upwards.

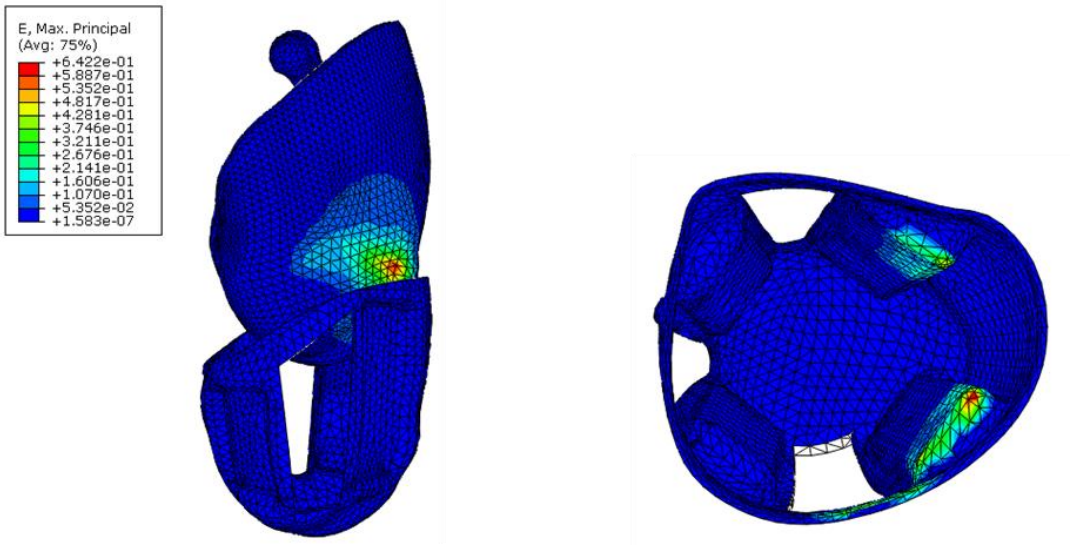

Figure 3.14 The simulation results for the CT image-based CRS socket. a, the donning simulation of the CRS socket; b, the contact stop area in the socket top view

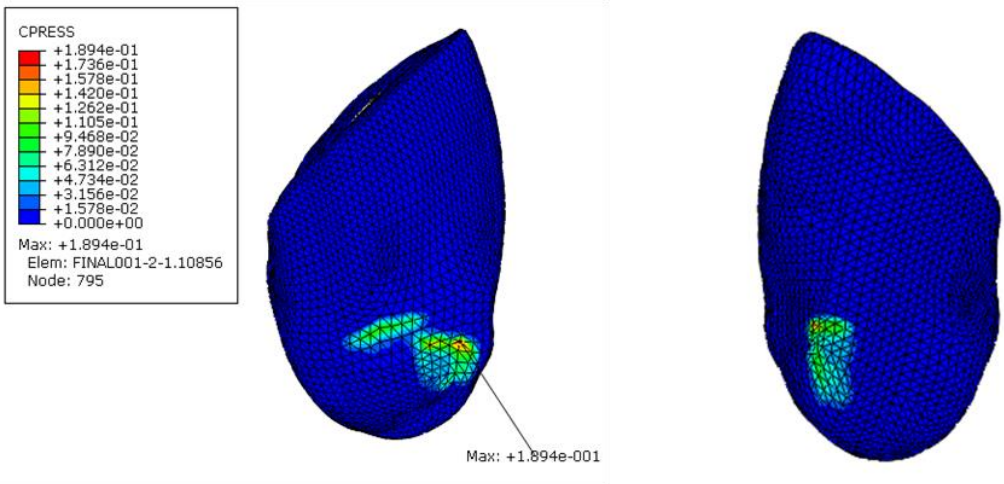

Figure 3.15 Normal stress (pressure) in MPa at the residual limb. a, the anterior-lateral side; b, the posterior-lateral side

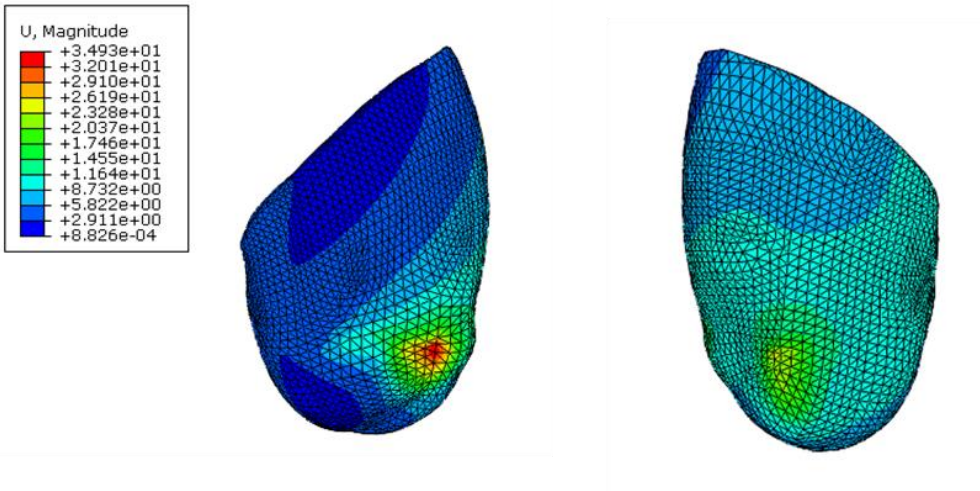

Figure 3.16 Displacement in millimeter at the residual limb. a, the anterior-lateral side; b, the posterior-lateral side

3.3.6 Summary

Plaster casting and 3D scanning were the two frequently used methods to get the residual limbs geometry (Andrysek, 2010). In either of these approaches, the residual limb has to keep in a good alignment position. It is important for the transfemoral residual limb to keep in the adduction position during casing or scanning (Schuch, 1988). However, this position prevents the 3D scanner to access the medial side of the transfemoral residual limb when the limb was in adduction. Some study selected an appropriate transfemoral brim from the computer database after the measurement of the patient's residual limb circumference (Travis, 1993). A specific CAD prosthetic system and software was required for this kind of method.

In this study, a CRS negative cast was taken first and then scanned it with the CAD system to achieve a more accurate geometry of residual limb. The designed casting apparatus had helped to achieve the goal. For further improvement, pressure sensors can be placed on the compression bars of the casting apparatus for the real-time adjustment of pressure.

The FE simulation result for CT-based amputee model could not be compared with other studies because it was aborted at forty percent of simulation. The difficulties on the convergence may be due to mesh conditions, material setting, or socket design. There were several attempts to adjust the mesh size and the non-linear operations but failed to fix the problems. However, the terminated results revealed some useful information. The maximum contact pressure was 189.4 kPa which larger than the literature for the transfemoral FE study. It was concentrated at the anterior-lateral side with some small contact pressure occurred at the posterior-lateral side. The anterior-medial side and posterior-medial side of the residual

limb did not contact with the socket. Therefore, the improvement of the CRS socket design should allow four compression areas to contact with the residual limb to redistribute the pressure initially.

The findings indicated that the edges of compression bars at the proximal area were too sharp which forced the compression pressure at the initial stage too concentrate on the horizontal plane to move the socket upward. The solution was to construct a smoother transition from the compression bars with the inner surface of the socket. It would approach the real situation, and the simulation of donning may be easier to converge.

The concept of using 3D reconstructed residual limb model to construct the CRS socket had the advantage of easy and accurate assembly and approved to be successful. Although the assemble simulation was not successful in our simulation, the important parameters for designing the CRS socket were identified during this process. The modification would be done to simulate the assembly successfully for the study in following chapter.

CHAPTER 4 ENHANCED FINITE ELEMENT MODELING

The study in chapter 3 had solved the difficulties in determining the compression depth and locations to construct a CRS socket model. Base on the study, 15mm compression was chosen for the recruited transfemoral amputee' CRS socket design. In order to increase the accuracy of FE, the formal study was utilized the 3D reconstructed MR image of the recruited transfemoral amputee's residual limb to build the CRS socket. The whole process was derived from the pilot study and improved based on the preliminary results.

The design of CRS socket for the subject was improved by making a smooth transient with the inner surface of the socket. The FE study focused on donning procedure, and 800N of subject's whole-body loaded. The interfacial stress and strain predicted by the FE model for 15mm compression CRS socket were compared with 10mm compression socket. In addition, the effect of coefficient of friction and silicone liner were studied.

4.1 Subject

A 48-year-old transfemoral amputee (Left side amputation) was recruited in this study. The patient got amputation 28 years ago due to the bone tumor and has been using the prosthesis since then. He is active in daily activities and walking every day using his prosthesis. There were no cardiovascular diseases and other health-related problems which contradicted to this study. The subject signed the informed consent before the experiment started. The Human Subjects Ethics Sub-committee in The Hong Kong Polytechnic University approved this research work (Reference Number: HSEARS20161011002).

The image of the subject's residual limb was taken from MRI system (GE Signa HDxt 1.5T, Canada). The slice thickness was set 2mm with 1mm gap, acquisition time 0.42s/35mins, matrix 320×160, Field of Vox 40×32cm (Figure 4.1). The patient was supine lying on the scanning gantry with the hip in the neutral position. The patient wore an unmodified plaster cast to minimize the gravity induced residual limb distortion. The protocol for conducting the MRI scanning was attached at the end (Appendix I). The segmentation of residual limb soft tissue and the bone was using MIMICS (Materialise, Belgium). Due to the limitation of view of the field, the MR image was separated into upper and lower parts. It combined to one identical residual limb structure by Boolean operation. The segmentation and 3D reconstruction were same as the pilot study 2.

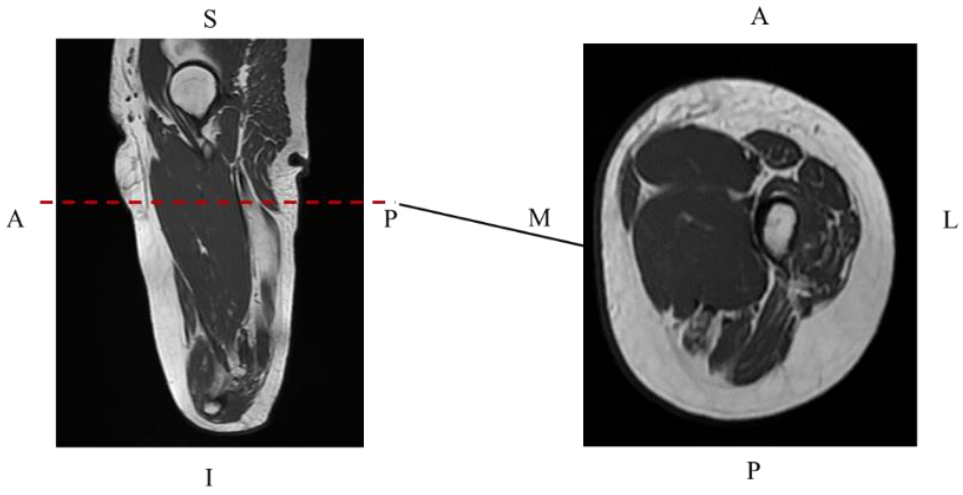

Figure 4. 1 The subject's MR image. Left, the lateral view; right, cross-section view

4.2 Development of transfemoral CRS socket using a 3D model

Most researchers built the socket model by scanning of the geometry of socket using the 3D scanner and then imported into SolidWorks for assembling and processing. It remains

challenging to assemble the socket and residual limb as they are in the different coordination. The study constructed the CRS socket using SolidWorks instead of commercially specific prosthetic CAD system to solve the problem. The method was quite same with the pilot study with the improvement of the CRS socket design based on the preliminary results.

Before starting the finite element analyzing, the first job was to create a CRS socket model. The critical point was to construct a successful CRS socket for the FEM. The frequently used method in the clinic is to rectify a positive plaster model based on a manual impression of the residual limb shape or use the computer software to modify 3D scanning geometry (i.e., Canfit^{TM}, VORUM). The former is subjective and relies on the clinical experiences; the latter, although it quantifies the modification value and less subjective, it is expensive and difficult to assemble the socket with soft tissue in the FE simulation.

The difficulties mentioned above were solved by the new method, which built the CRS socket based on the 3D reconstructed residual limb geometry. It needed to modify the socket design to make a smoother transient at the compression protrude areas based on the pilot study. The socket was constructed by offset the surface of the 3D geometry of residual limb in SolidWorks. The compression was started 40mm below the upper brim of the socket. Four compression areas with an equal width were centered between the median sagittal and median coronal plane with the adjacent openings for tissue displacement. The compression depth was set 15mm, which was decided in chapter 3. In order to compare compression depth effects, a 10mm compression value CRS socket was created as well.

The sketching of CRS socket was started at setting the two-orthogonal plane (plane 1 and plane 2) to initiate the 45 degrees. Plane 1 was created first by setting a new plane passing through the center of the socket and formed 45 degrees with the middle of the top plane. Plane 2 was created by setting a new plane orthogonal to the first one. On plane 1 and plane 2 of the socket surface, four straight lines of 15mm lengths were sketched. The width (50mm) and thickness (15mm) were drawn on the front plane. By employing the surface-sweep function, the compression shape was formed automatically (Figure 4.2).

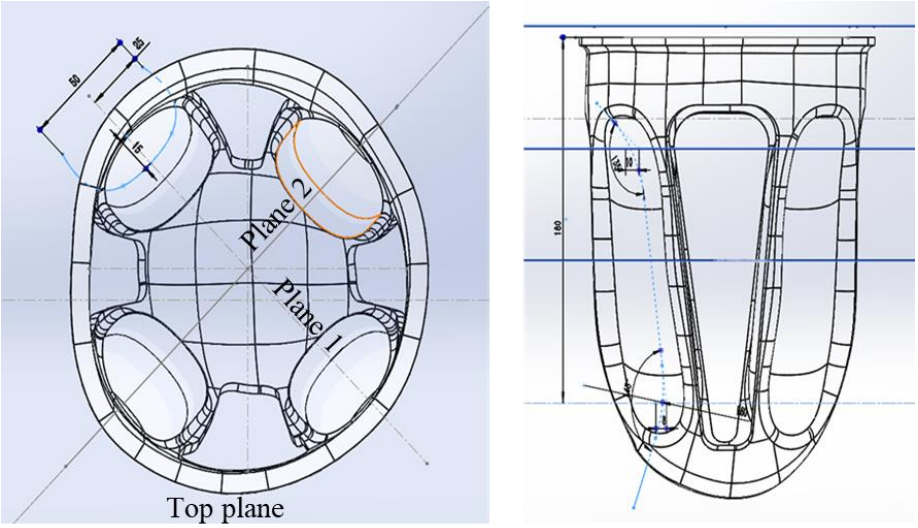

Figure 4. 2 CRS socket design in SolidWorks. Left, the top view; Right, the frontal view

The creating of openings between adjacent compression bars was done using the split line function. Round corners were adopted. There were 8 degrees of fillet on the brim of the socket to avoid pinching the soft tissues. The CRS socket was then created by thickening the offset surface 4mm.

The created CRS socket can be exported to STL file for 3D printing. The existing 3D printing materials are hardly to fulfill prosthetic socket's strength and heating-modification requirement. Therefore, this study selected the CAM milling method. The positive STL model was built by using the 3D soft tissue model subtracting the socket geometry. The file was then sent to Prosthetics and Orthotics Department, Prince of Wales Hospital for CAM milling. The whole process from the 3D reconstruction of the residual limb to the CAM milled CRS foam model shows in Figure 4.3.

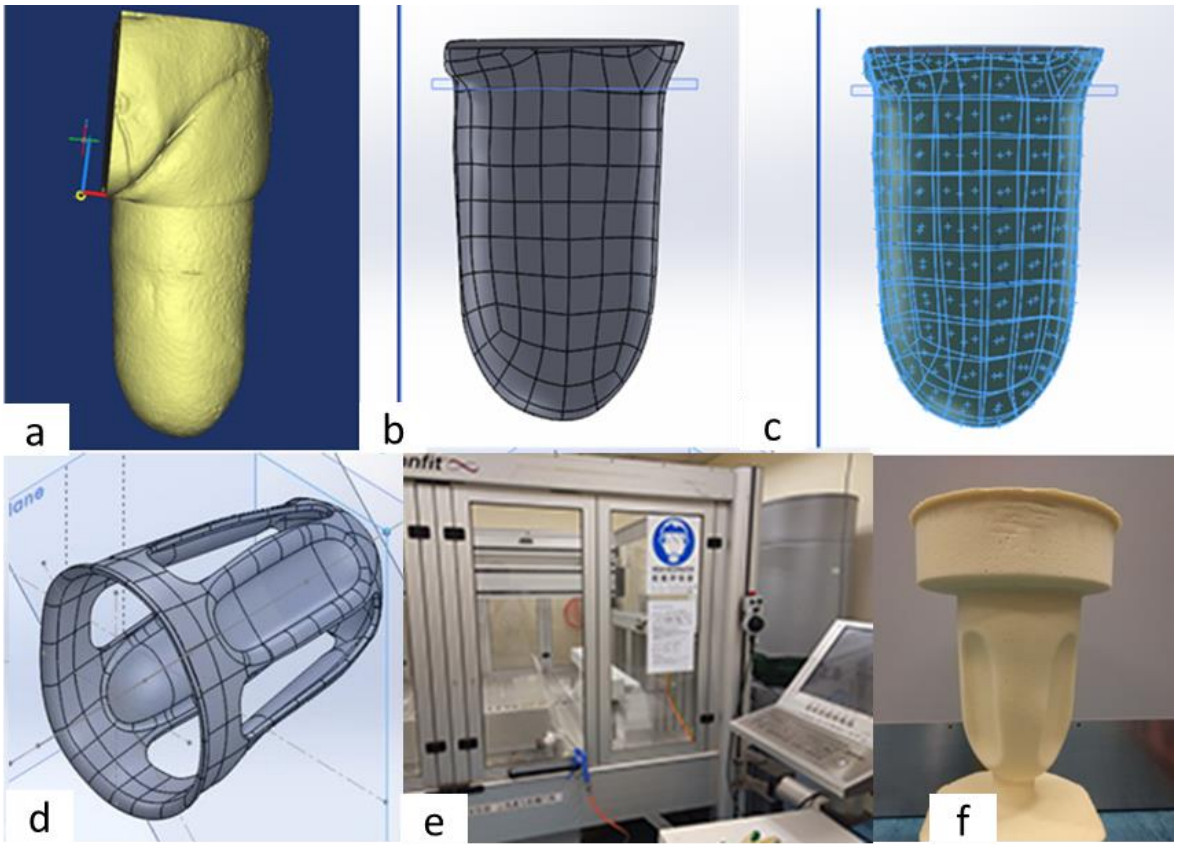

Figure 4. 3 The flowchart of CRS socket design from 3D reconstruction to positive model. a, the 3D reconstruction of residual limb geometry by mimics; b, the 3D residual limb soft tissue was imported into SolidWorks for design of CRS socket and assembly; c, offset outer surface of the residual limb to obtain the socket cast; d, finished CRS socket; e, CAM machine for milling; f, the computer-aided manufactured positive CRS model ready for thermoforming

The CRS socket was thermoformed by using 15mm thickness ThermoLyn rigid plastic sheet (polystyrene, OTTO BOCK, German) (Figure 4.4).

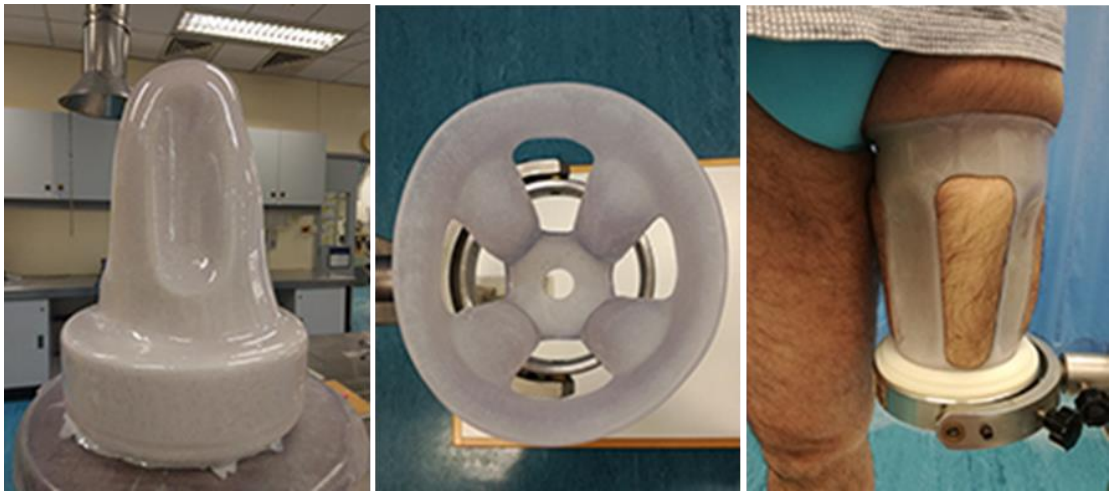

Figure 4. 4 Right, thermoforming of the CRS cast; middle, CRS socket; right, CRS socket fitting

4.3 Simulation with the inclusion of a silicone liner

The opening structure of the CRS socket makes the traditional suction suspension difficult to be achieved. The silicone liner was adopted for the suspension. The prosthetic silicone liner not only helps to protect the skin but redistribute the load (Klute et al., 2010). A silicone liner was built according to the geometric of the 3D constructed residual limb. It supposed to reduce the stress and strain. The results were compared with the socket without the silicone liner. The outer surface of the 3D model was offset 0mm same as the base of CRS socket built. 3mm thickness was added to this offset surface to represent a 3mm silicone liner. The silicone liner was assembled with soft tissue. A CRS socket was constructed. The bone, soft tissue, silicone liner and CRS socket were assembled in the SolidWorks (Figure 4.5). During

the assembly, the residual limb and liner were fixed. The socket was only allowed to move in the Z direction and stopped at initial contact with the residual limb. The displacement was measured for the residual limb and socket's front plane.

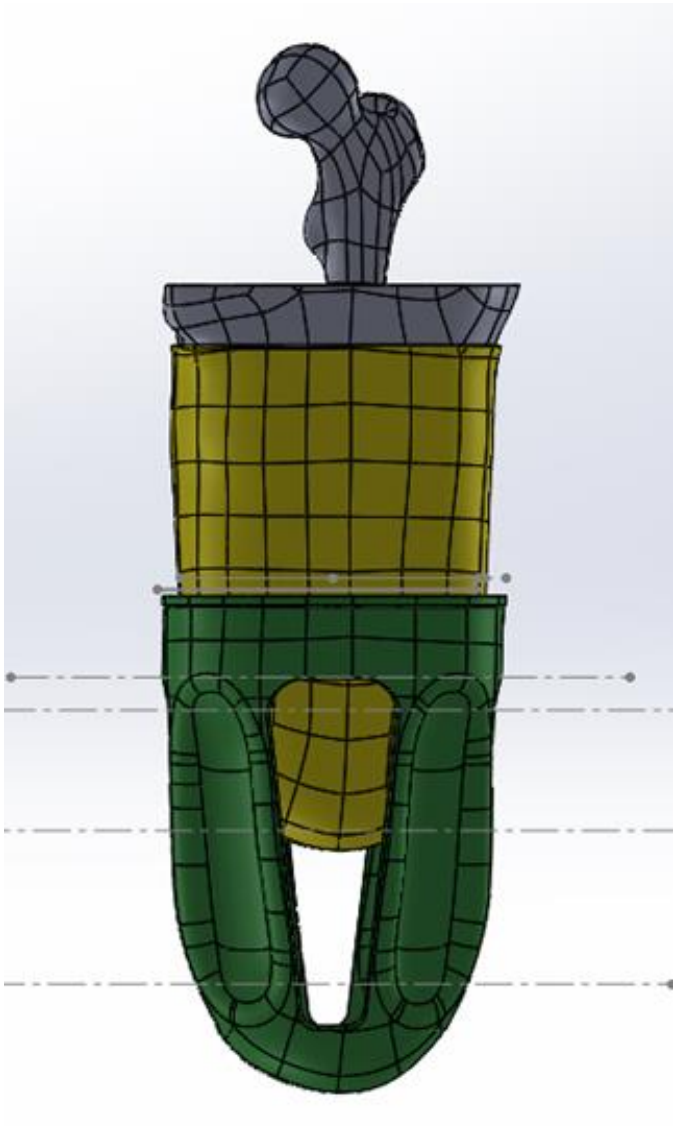

Figure 4. 5 The assembly of the residual limb (gray), liner (yellow) and CRS socket (green)

4.4 Development of finite element model

4.4.1 Material properties

The material properties of the bone, soft tissue and socket were assumed to be linear elastic, homogeneous and isotropic. The 3D tetrahedral (C3D4) mesh elements were set for all materials to reduce the computational cost. The element size was 3mm for bone and socket and silicone liner, 5mm for the soft tissue. There were total 349828 elements for the model without liner and 4565797 with liner. The detailed properties are shown in Table 4. 1.

Table 4. 1 Material properties and FE model detail

Material properties			FE model mesh details			
Material	**Young's modulus (Mpa)**	**Poisson's ratio**	**Node distance (mm)**	**Elements**	**Total elements**	**Element type**
Bone	15000	0.3	3	58982	349828	C3D4
Tissue	0.2	0.49	5	166663		
Socket	1500	0.3	3	124183		
Silicone liner	0.4	0.39	3	115969		

The literature reported the coefficient of friction between the skin and polypropylene ranging from 0.188 to 0.545 (Restrepo, 2014). A coefficient of 0.415 was chosen by (Lacroix & Patiño, 2011) and Veleza et al. (2015) in the FE study of the transfemoral prosthetic socket. Therefore, the coefficient of friction between the residual limb and socket was set 0.4. Additionally, values of 0.3 and 0.5 were also selected to examine the effect of coefficient of friction for the socket without the liner. The coefficient of friction between the outer surface

of the silicone liner and socket was set 0.4, and 0.5 for the inner surface of silicone liner and residual limb (Zhang, 2013).

4.4.2 Boundary conditions and load

The interaction between the soft tissue and socket was a surface-to-surface contact. The harder property of the socket was defined as master surface whereas the outer surface of soft tissue was slave surface. This structure prevents the penetration of the master nodes into the slave surface. Femur and soft tissue were tied as one body part. The simulation was implemented by software Abaqus 6.11 (Dassault Systèmes, RI, USA). The assembled meshed bone, soft tissue, silicone liner and CRS socket shows in Figure 4.6.

Figure 4. 6 The meshed bone, soft tissue, silicone liner and CRS socket were assembled

The whole simulation was divided into two steps: (1) donning procedure of prosthesis, (2) loading effect by the subject's whole-body weight.

In the donning process, a 106mm upward displacement of the prosthetic socket was given while fixing the femoral head in all directions (Figure 4.7, a). In the loading process, an 800N force which was around the subject's whole-body weight applied at the femoral head with the constraint of the distal end of the socket (Figure 4.7, b).

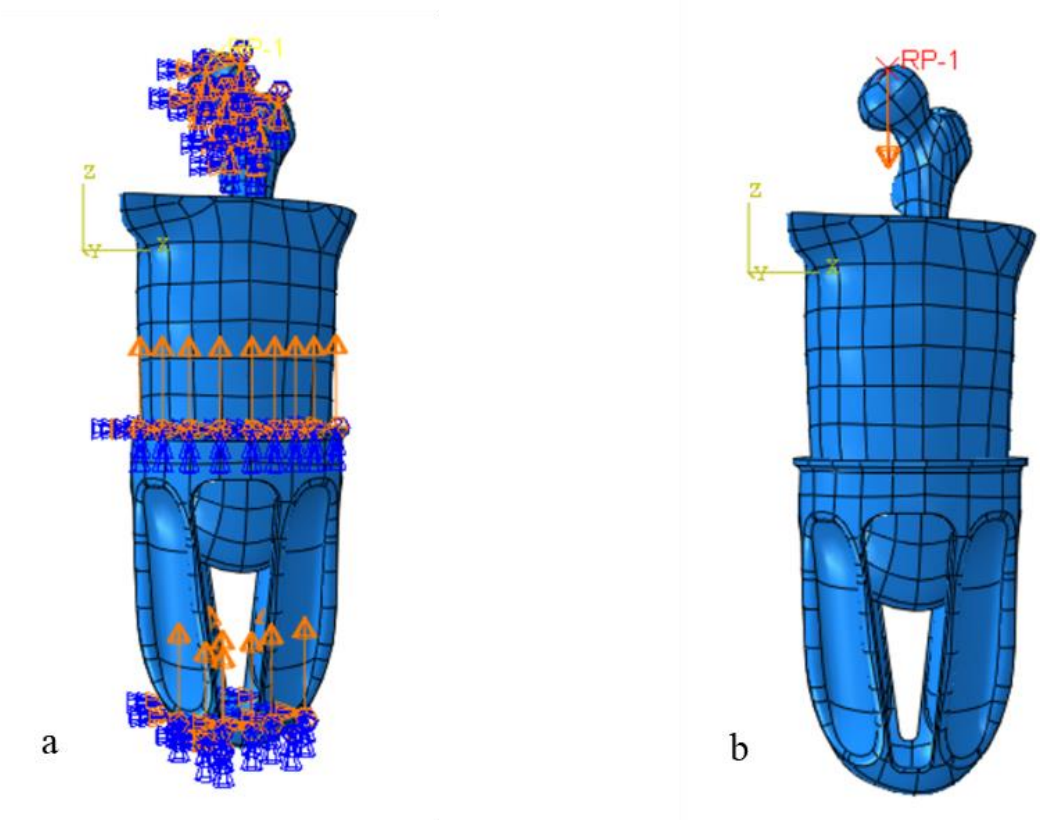

Figure 4. 7 a, the boundary condition in the first step, 106mm upward displacement of CRS socket with the fixation of the femoral head; b, the second step, 800 Newton around the subject's body-weight applied on the femoral head with the displacement remained.

4.5 Experimental validation

Experimental validation was done by using F-scan system (Tekscan Inc., Boston, USA). The sampling frequency was set at 50Hz. The sensor was put between the residual limb and socket and attached on the compression bars by double-sided adhesive tape. The sensor was calibrated according to the patient's body weight and according to manufacturer's instructions. Two corresponding counter-anticounter sides were measured each time. After donning the socket, the patient was allowed to have 10 minutes to accommodate the prosthetic socket. The prosthetist slowly adjusted the supporting of the CRS socket to ensure the pelvis level. The patient lifted his sound side leg and utilized the amputated side to support (Figure 4.8). The sound side of the patient's upper limb firmly supported on an elbow crutch in case loss of balance. Three successive trials were performed while the patient lifted the sound side. One minute was allowed for the subject to rest during each trial. The subject filled developed questionnaire after the pressure measurement.

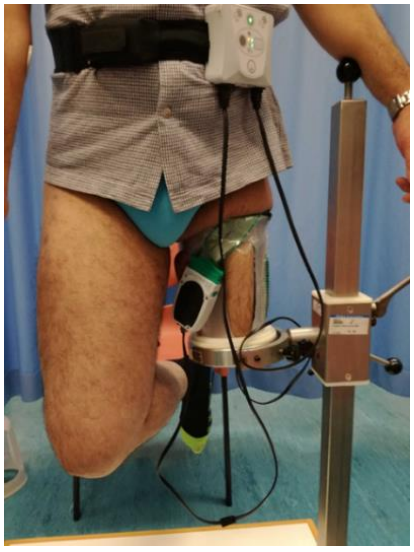

Figure 4. 8 the pressure sensor validation of the CRS socket while the patient full body weight added

CHAPTER 5 RESULTS

5.1 Stress and displacement in the donning procedure

The FE predicted von Mises stress, contact pressure, and displacement are shown in Figure 5.1, 5.2, and 5.3 respectively. The maximum von Mises stress and peak contact pressure was 227.7 kPa and 254.1 kPa respectively (Figure 5.1, Figure 5.2). The maximum displacement was 59.27mm (Figure 5.3).

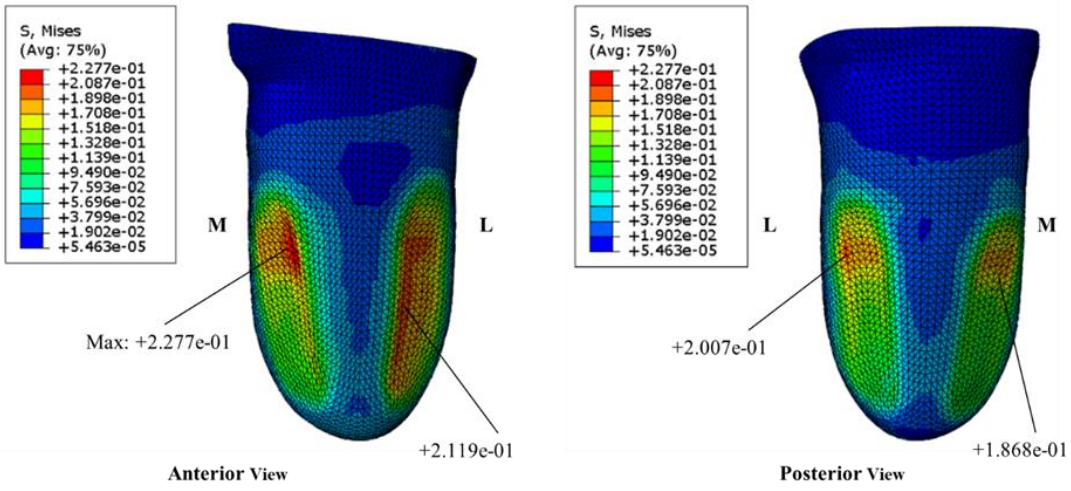

Figure 5. 1 The FE predicted von Mises stress (MPa) on the residual limb distribution at CRS socket donning

The contact pressure distribution on the residual limb revealed mostly green and smooth. It may suggest a uniform contact between the compression bars and the residual limb surface. The maximum von Mises stress for the individual bar was concentrated at the proximal part

of compression areas except for the posterior-lateral area at which the maximum stress distributed along the whole compression area and spread from the center. The differences were likely caused by the distance of the compression surface to the femur bone and the soft tissues around it. From the cross-section view of the residual limb, the soft tissues (fat and muscles) are close to the shaft of the femur in the anterior-lateral side while at other three directions around the femur, the soft tissues around the femur are thicker. Thicker soft tissue can cause more displacement and more energy absorption. It was verified by the displacement results of the residual limb. The maximum displacement was 59.27mm at proximal posterior-medial side. The posterior-lateral side was 53.2mm and 52.2mm for the anterior medial side. All values were considerably higher than 38.3mm in the anterior-lateral side.

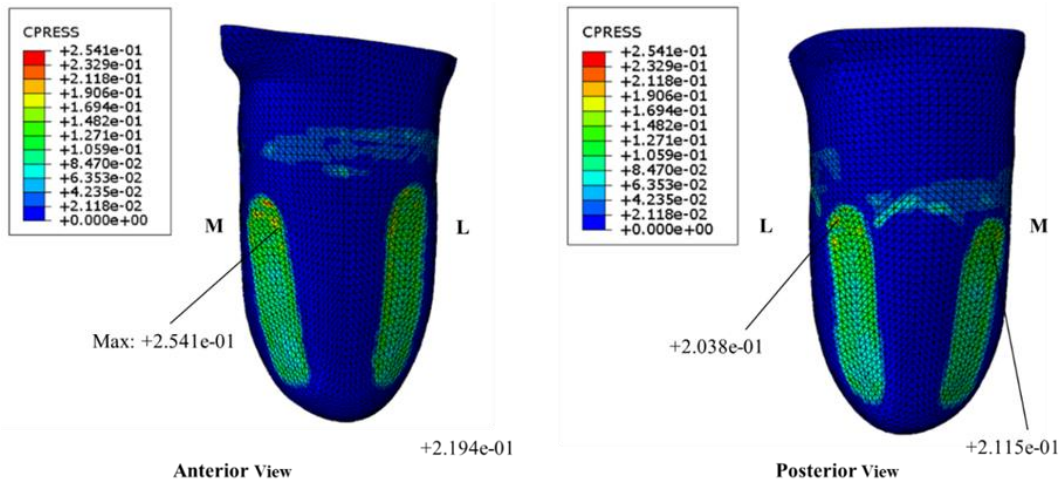

Figure 5. 2 The predicted contact pressure (MPa) distribution on the residual limb at CRS socket donning

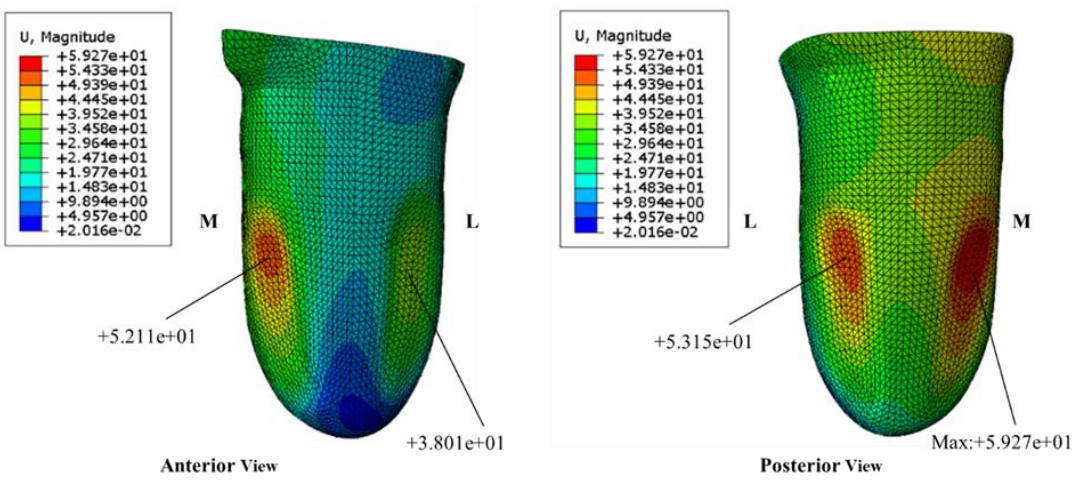

Figure 5. 3 The predicted displacement (millimeter) on the residual limb at the CRS socket donning

5.2 Stress and displacement after vertical load applied

The maximum von Mises stress was 191.9 kPa, 218.5 kPa for the contact pressure both shown in the anterior-medial side (Figure 5.4, Figure 5.5), whereas the maximum displacement was 59.32mm on the posterior-medial side (Figure 5.6). The locations and pressure did not change much after the vertical load applied. However, all the values were decreased.

Although 800N vertical load added at the femoral head, the maximum von Mises and peak contact pressure were both decreasing compared with donning procedure. This probably because more soft tissues contacted with the socket when the body weight applied which increased the contact areas of the compression. The von Mises stress, contact pressure and the displacement distribution pattern were similar to donning procedure.

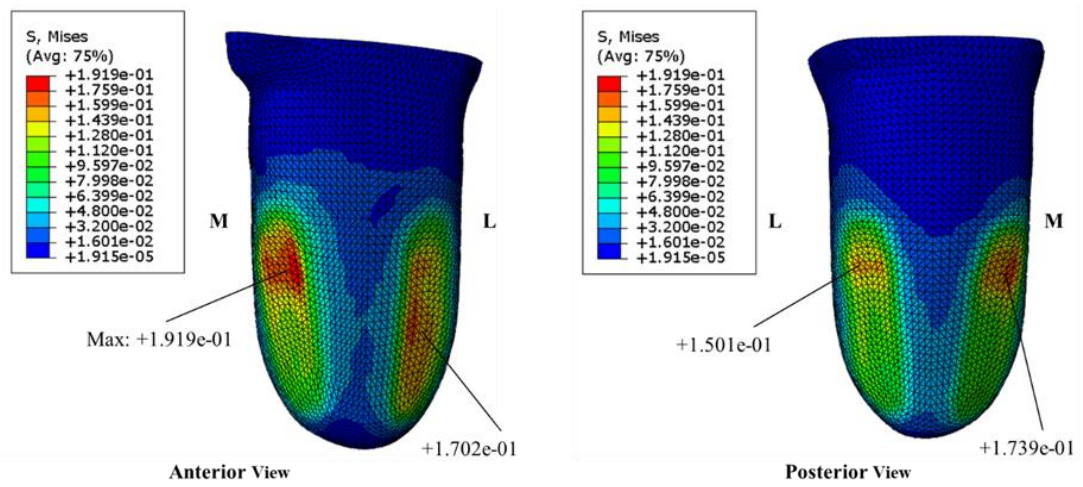

Figure 5. 4 The predicted von Mises stress (MPa) distribution on the residual limb after 800N vertical load applied

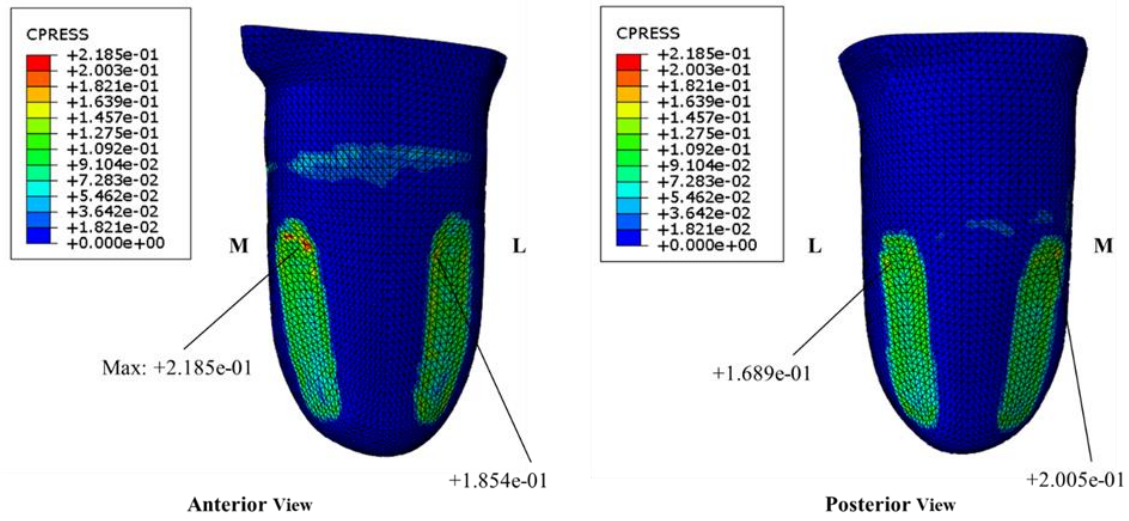

Figure 5. 5 The contact pressure (MPa) distribution on the residual limb after the 800N vertical load applied

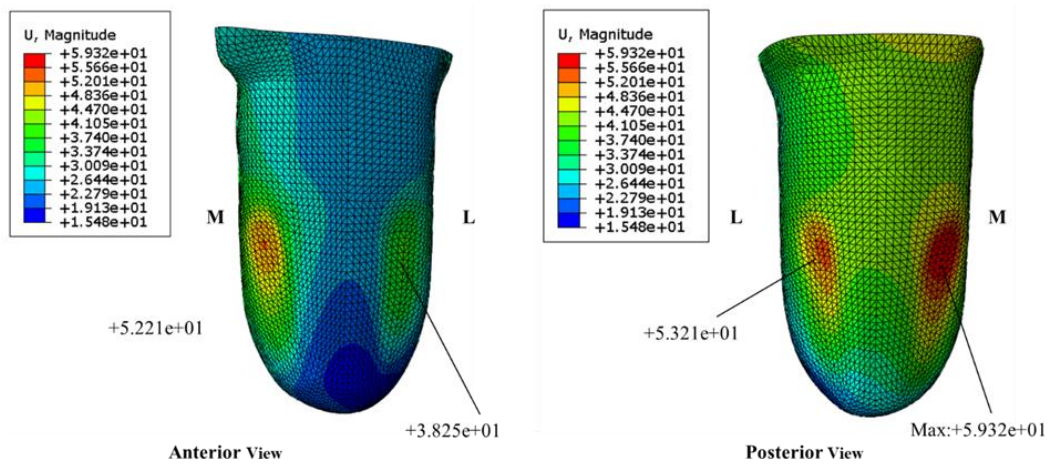

Figure 5. 6 The FE predicted displacement (millimeter) of residual limb after the 800N vertical load applied

5.3 Stress and pressure distribution at different compression location

Figure 5.7 shows the von Mises stress value at different compression areas in the donning and 800N vertical load adding procedure. The maximum stress occurred at the anterior-medial side in both steps followed was the anterior-lateral side at donning process 212 kPa, but 171 kPa in the posterior-medial side while vertical load added. The third one was 201 kPa in the posterior-lateral at donning procedure and 170 kPa in the anterior-medial side while vertical loading applied. The last was 187 kPa in the posterior-medial side at donning procedure and 151 kPa in the posterior-lateral side while loading added. The difference between the maximum and minimum in the donning procedure and vertical load apply was 41 kPa and 40 kPa respectively. The stresses decreased from the donning procedure to loading process about 16.2% in the anterior-medial side, 19.8% in the anterior-lateral side, 8.5% in the posterior-medial side and 24% in the posterior-lateral side.

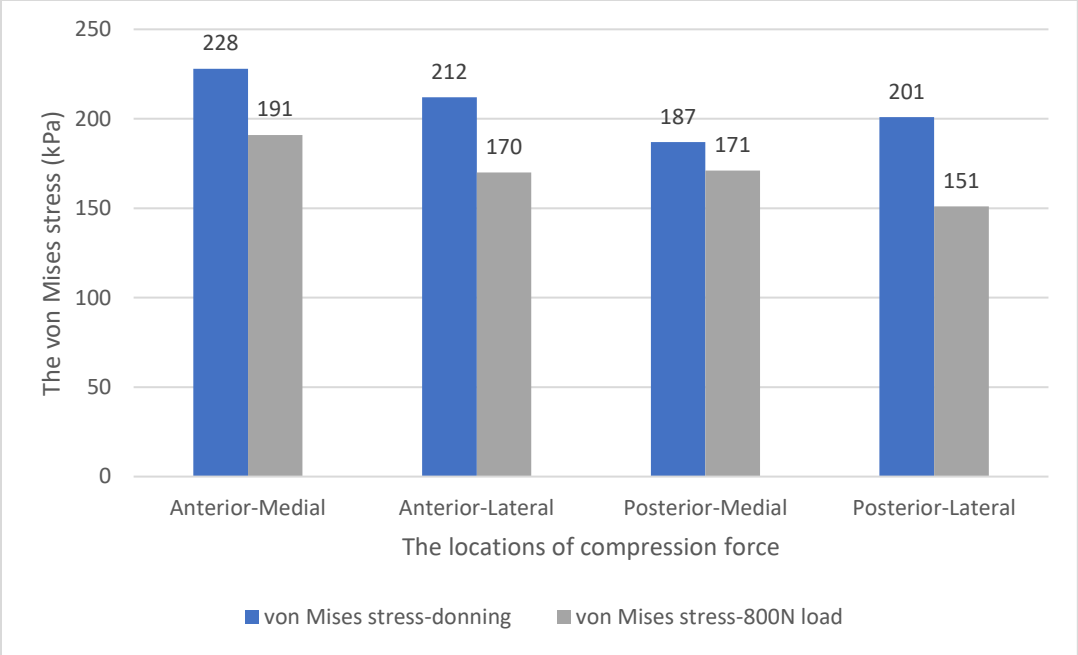

Figure 5. 7 The von Mises stress at the donning and after 800N vertical load applied

The displacement is the three-dimensional movement of an element in the x, y, and z-direction. The strain reflects the deformation of an object. They are related to tissue's property and orientation. The strain of the residual limb in this study shows the similar pattern with the von Mises stress where the maximum deformation occurred at the maximum von Mises stress (Figure 5.8).

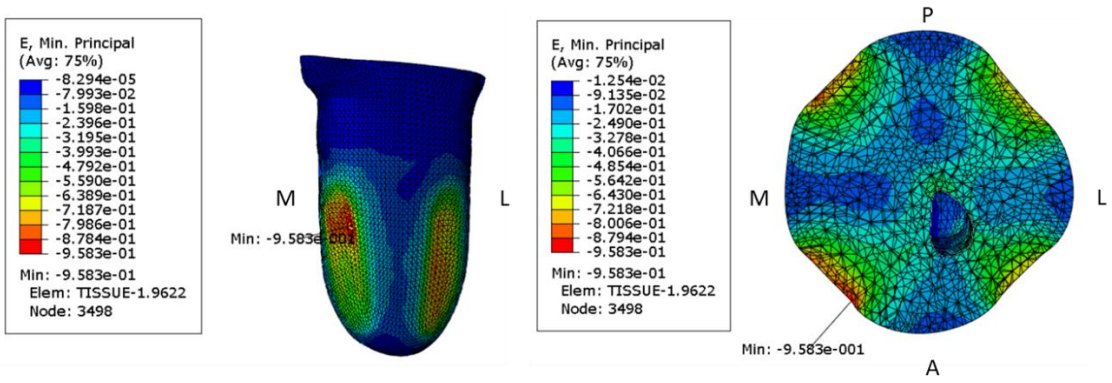

Figure 5. 8 The strain of the residual limb. Left, the anterior view; right the cross-section view

Figure 5.9 shows the contact pressure at different compression areas in the donning and 800N vertical load adding procedure respectively. The maximum compression occurred at the anterior-medial side in both steps followed was the anterior-lateral side in donning procedure 219 kPa, but 200 kPa in the posterior-medial side while loading added. The third one was 212 kPa in the posterior-medial side at donning procedure and 185 kPa in the anterior-lateral side while vertical loading applied. The last was 204 kPa in the posterior-lateral side at donning procedure and 169 kPa in the posterior-lateral side while loading added. The difference between the maximum and minimum in the corresponding areas of donning procedure was 50 kPa, 49 kPa while the loading applied. The stresses decreased from the donning procedure to loading process about 14.2% in the anterior-medial side, 15.5% in the anterior-lateral side, 5.7% in the posterior-medial side and 17.2% in the posterior-lateral side.

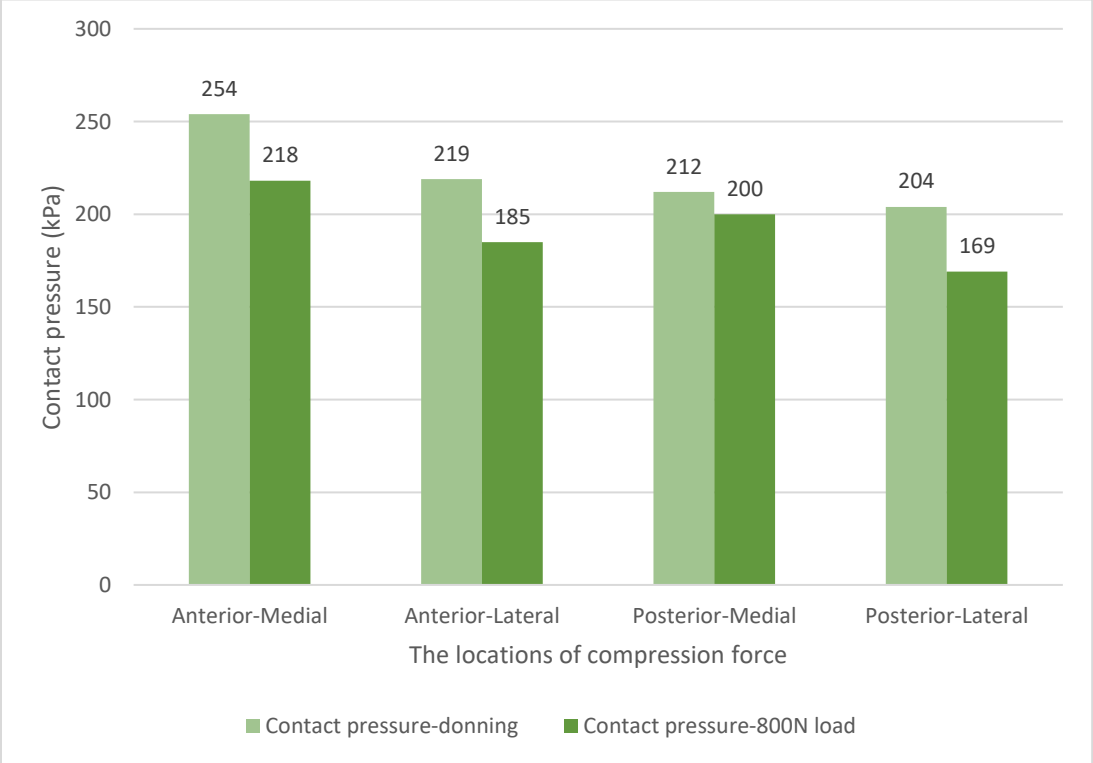

Figure 5. 9 The compression pressure in the donning and vertical load adding procedure

5.4 Effects of the coefficient of friction

Table 5.1 shows the effect of different coefficient of friction on the von Mises stress, contact pressure and displacement.

Table 5. 1 The results of von Mises stress, contact pressure and displacement predicted by the FE model on different coefficients of friction

	Donned procedure			Vertical load applied (800N)		
Friction (μ)	von Mises stress	Contact pressure	Displacement	von Mises stress	Contact pressure	Displacement
	kPa		mm	kPa		mm
0.5	261	324.9	67.68	206.8	298.2	67.77
0.4	227.7	254.1	59.27	191.9	218.5	59.32
0.3	194.3	219.4	50.89	172.1	212.9	50.92
	% The percentage of parameters difference under different coefficient of friction					
$(f_{0.4}-f_{0.5})/f_{0.5}$	-12.76%	-21.79%	-12.43%	-7.21%	-26.73%	-12.47%
$(f_{0.3}-f_{0.4})/f_{0.4}$	-14.67%	-13.66%	-14.14%	-10.32%	-2.56%	-14.16%

In the donning procedure, all the parameters decreased while the coefficient of friction decrease. The von Mises stress decreased from 261 kPa to 227.7 kPa, with a 12.76% reduction for the friction from 0.5 to 0.4; and from 227.7 kPa to 194.3 kPa, with an 14.67% reduction from the coefficient of friction from 0.4 to 0.3 respectively. Nevertheless, the contact pressure increased from 213 kPa to 216.8 kPa, with a 1.78% increment for the friction from 0.5 to 0.4; and from 216.8 kPa to 187.7 kPa, with a 13.42% reduction from the coefficient of friction 0.4 to 0.3.

After the 800N applied, the von Mises stress decreased from 206.8 kPa to 191.9kPa, with a 7.21% reduction for the coefficient of friction from 0.5 to 0.4; and from 191.9 kPa to 172.1kPa, with a 10.32% reduction for the coefficient of friction from 0.4 to 0.3. The contact pressure decreased from 298.2 kPa to 218.5 kPa, with a 26.73% reduction for the friction

from 0.5 to 0.4; and from 201.5 kPa to 187 kPa, with a 2.56% reduction from the coefficient of friction 0.4 to 0.3.

In these two steps, the von Mises stress were not decreased significantly compared with the contact pressure with changing the coefficient of friction. Especially when the coefficient of friction changing from 0.5 to 0.4, the contact pressure was decreased dramatically. It may be an indication that the contact pressure was more sensitive for a coefficient of friction above 0.4.

The displacement in the donning and vertical load applied steps decreased within the range around 12% to 14% respectively when the coefficient of friction decreased 0.1. The displacement decreased slightly larger for a smaller coefficient of friction.

5.5 Effects of compression depth and silicone liner

Table 5.2 shows the results of von Mises stress, contact pressure and displacement predicted by the FE model regarding the CRS socket compression depth 15mm and 10mm, no liner and with liner conditions.

In the donning procedure, the von Mises stress and contact pressure were 227.7 kPa and 254.1 kPa respectively for the 15mm depth, 170.9 kPa and 216.8 kPa for the 10mm depth compression. Compared with 15mm depth compression, the von Mises stress and contact pressure decreased 24.95% and 14.68% respectively. The using of silicone liner reduced the contact pressure 41.37%.

Table 5. 2 The results of von Mises stress, contact pressure and displacement predicted by the FE model comparing CRS socket with 10mm and 15mm compression depth, with and without liner

Condition	Donning procedure			Vertical load applied (800N)		
Compression depth (mm)	von Mises stress	Contanct pressure	Displacement	von Mises stress	Contanct pressure	Displacement
	kPa		mm	kPa		mm
10	170.9	216.8	45.49	155.8	201.5	45.51
15	227.7	254.1	59.27	191.9	218.5	59.32
No liner/with liner						
No liner	170.9	216.8	45.49	155.8	201.5	45.51
With liner	138.4	127.1	41.53	114.4	125.9	41.65
	% The percentage of parameters difference under condition					
$(C_{10d} - C_{15d})/C_{15d}$%	-24.95%	-14.68%	-23.25%	-18.81%	-7.78%	-23.28%
$(W_{liner} - No_{liner})/W_{liner}$%	-19.02%	-41.37%	-8.71%	-26.57%	-37.52%	-8.48%

KEY: C_{10d} =10mm compresssion, C_{15d} =15mm compression; W_{liner} = with liner model, No_{liner} = No liner model

After the 800N vertical load applied, the contact pressure reduced 7.78% for the compression depth from 15mm to 10mm while it generated a 37.52% of reduction by using a silicone liner than without the liner. The using of silicone liner reduced the contact pressure around 40% in both stages. This value was considerably higher than reducing the compression depth.

With the silicone liner, the displacement of the soft tissue was reduced nearly 9% in donning and the 800N vertical loading condition. Around 23% reduced in 10mm compression depth socket. The results may suggest that compared with the depth reduction, using the silicone liner was more effective on the contact pressure reduction, which can protect the soft tissue bearing the high pressure. However, it caused more soft tissue displacement than a 5mm compression depth reduction.

The shear stress was found to be near linearly proportioned with the changing of the coefficient of friction (Figure 5.10).

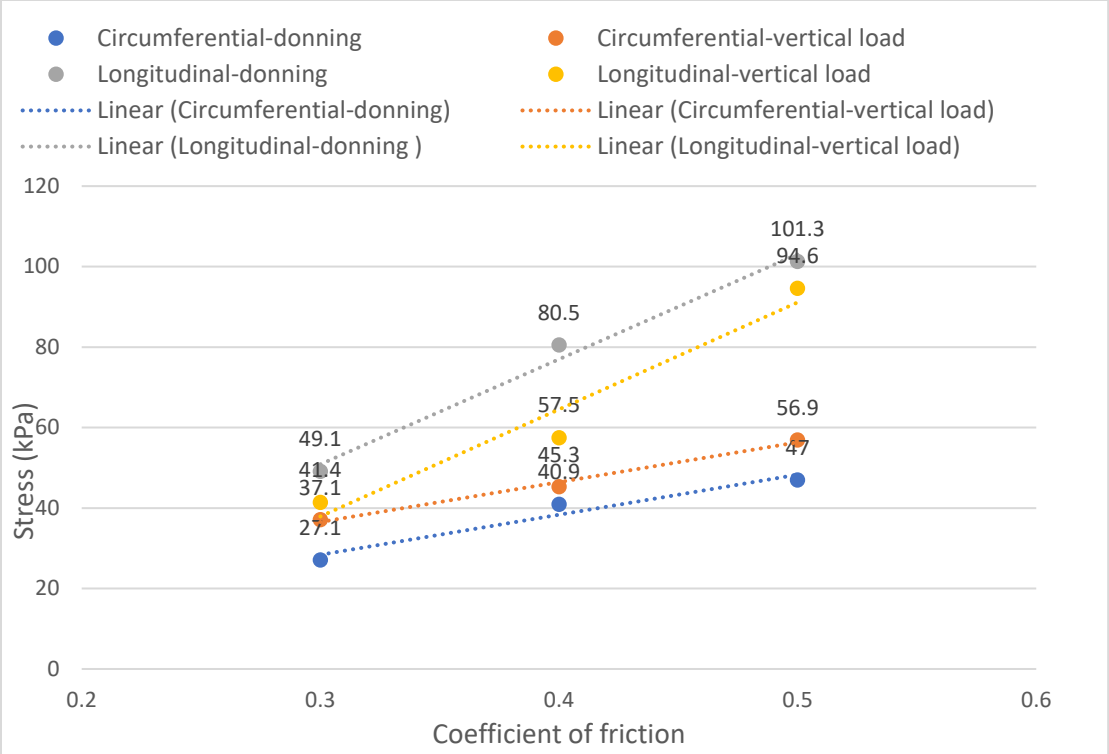

Figure 5. 10 The Shear stress with a different coefficient of friction at donning and 800N vertical load

5.6 The validation results

In the experimental validation, the maximum compression pressure measured at the anterior-lateral side was 239 kPa. It was 21 kPa larger than the maximum value of FE prediction but at a different site. The maximum measured value was 54 kPa lager than the FE simulation results at the same compression area (Figure 5. 11). At the other three compression locations, they were all lower than the predicted results (Figure 5. 12). It was possible that the elbow crutch supported partially of the patient's body weight during the measurement.

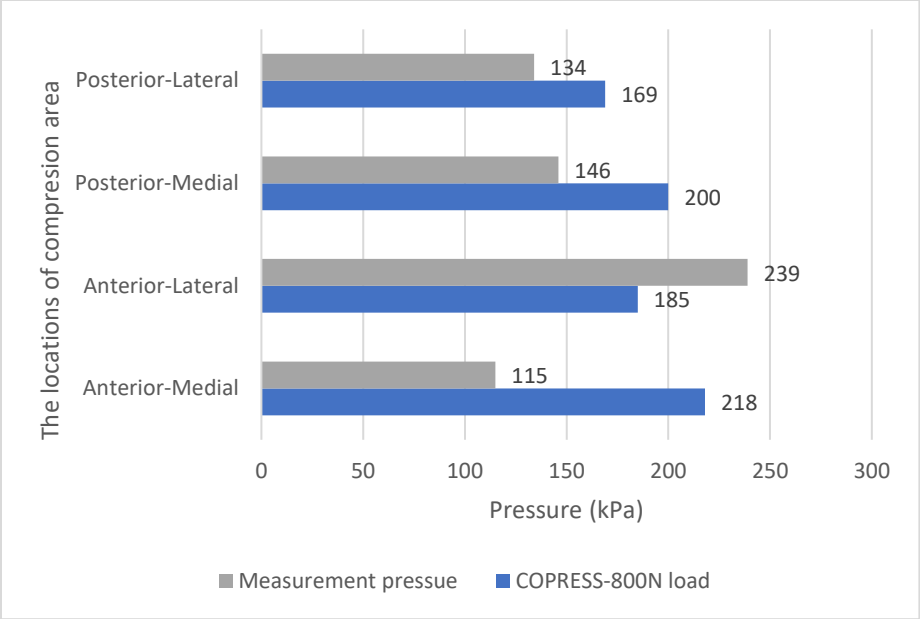

Figure 5. 11 The FE simulated compression pressure and experimental results

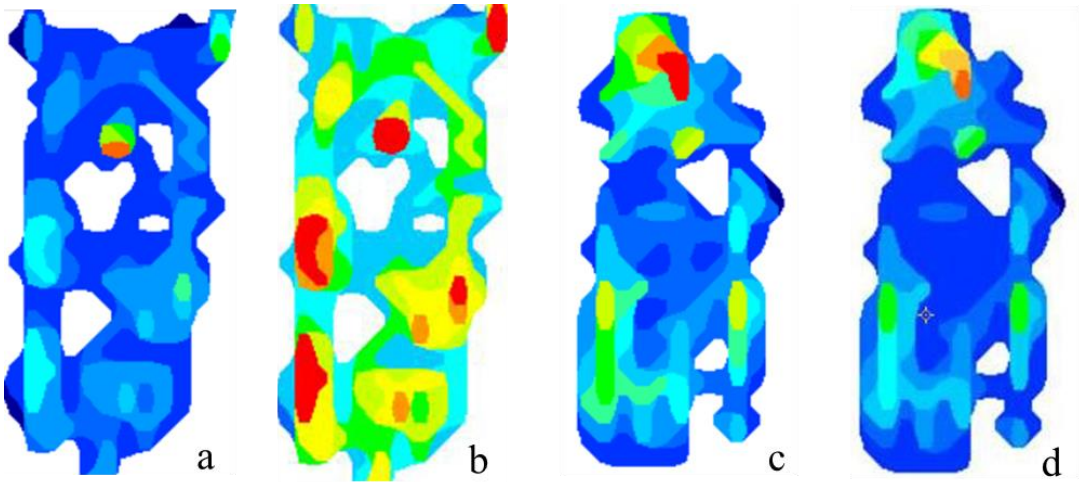

Figure 5. 12 The measurement pressure distribution results. a, anterior-medial area, b, anterior-lateral area, c posterior-medial area, d, posterior-lateral area

CHAPTER 6 DISCUSSION

6.1 Maximum contact pressure on the residual limb

In recent FE studies on transfemoral amputee (Table 6. 1), the maximum contact pressure was 200 kPa as reported by Colombo et al., (2014). The peak contact pressure in this study was 218 kPa, which was slightly smaller to their work on the transfemoral amputee. Colombo et al. evaluated the condition during the gait. It would be much smaller if it conducted under the static vertical load condition, as during the gait the body-weight applied at the hip joint was several times bigger. Therefore, our results will be larger than that one if it would be conducted under the same condition. Velez et al. (2015) found the maximum pressure during donning and loading with Quad and IRC socket designs was 151 kPa from one transfemoral amputee. Their result was 30% smaller than this study. The compression force in the CRS socket was much higher than the maximum pressure in conventional socket designs.

Table 6. 1 The FE simulation results for the lower limb prosthetic socket extracted (Dickinson, 2017)

Reference	Content	Friction	Maximum pressure (kPa)	Maximum shear stress (kPa)	Level
Veleza et al., 2015	Pre-load and static loading	0.415	151	55	Transfemoral
Restrepo et al., 2014	Strip COF 0.2 and global COF 0.9	0.2-0.6	70	N/A	
Colombo et al., 2014	The contact pressure at residual limb interface during different gait	0.4	200	N/A	
Zhang et al., 2013	50N simulate pre-loading	0.5	119	longitudinal 104; cicumferential 25.65	
Lacroix and Patino 2011	Socket donning by brim displacement	0.415	5.61	longitudinal 0.93; cicumferential 1.48	
Zhang and Roberts, 2000	FE simulation and validation	0.5	90	50	Transtibial
Zachariah and Sanders, 2000	Interface stress prediction	0.675	201.5	33.2	
Wu et al., 2003	Interface presure and pain-pressure tolerance	0.5, 0.6	250	130	
Jia et al., 2005	Interface pressue and shear stress between socket and residual limb	0.5	340	85	
Lee et al., 2004	Interface stress under the rectification	0.5	185	67	
Lin et al., 2004	Liner stiffness on the interface pressure	0.5	783	373	

The results of compression depth on the 10mm and 15mm compression showed that with the compression depth increased by 5mm there were 8% and 15% pressure increased in the donning and loading procedure respectively. Additionally, the predicted (218 kPa) and measured (239kPa) values were much lower under pain threshold (310 kPa to 600 kPa) and pressure tolerance range (400 kPa to 910 kPa) reported by (Lee, 2005) on the transtibial amputees. However, the sensitivity and pressure tolerance of the transfemoral and transtibial residual limbs may be different. There has been no report on the pain threshold and tolerance of the transfemoral residuum. Moreover, there is only one femur bone well protected by soft tissues in the thigh it is likely that the transfemoral amputee will be more tolerable for the CRS design.

The locations of the peak pressure predicted by the FE model and that measured in the experiment were not matched. In the experimental measurement, the maximum pressure located at the anterior lateral side at which there were minimum soft tissues surrounding the femur bone. Previous study found that the thicker the soft tissue, the lower the peak impact force, and the higher the energy was absorbed (Robinovitch et al., 1995). Therefore, the maximum compression force should occur at the location with the least soft tissue around the femur bone. The location in this study was the anterior-lateral side. It was consistency with the F-scan measurement result but not matched with the FE simulation. It may be that in the FE model, the downward vertical force was directly added to the top of the femoral head which was closer to the anterior-medial side of the residual limb. The downward force from the femoral head generated an anticlockwise momentum exerted on the femoral shaft, which enabled the proximal anterior-medial and distal anterior-lateral soft tissue experiencing further compression (Figure 6. 1).

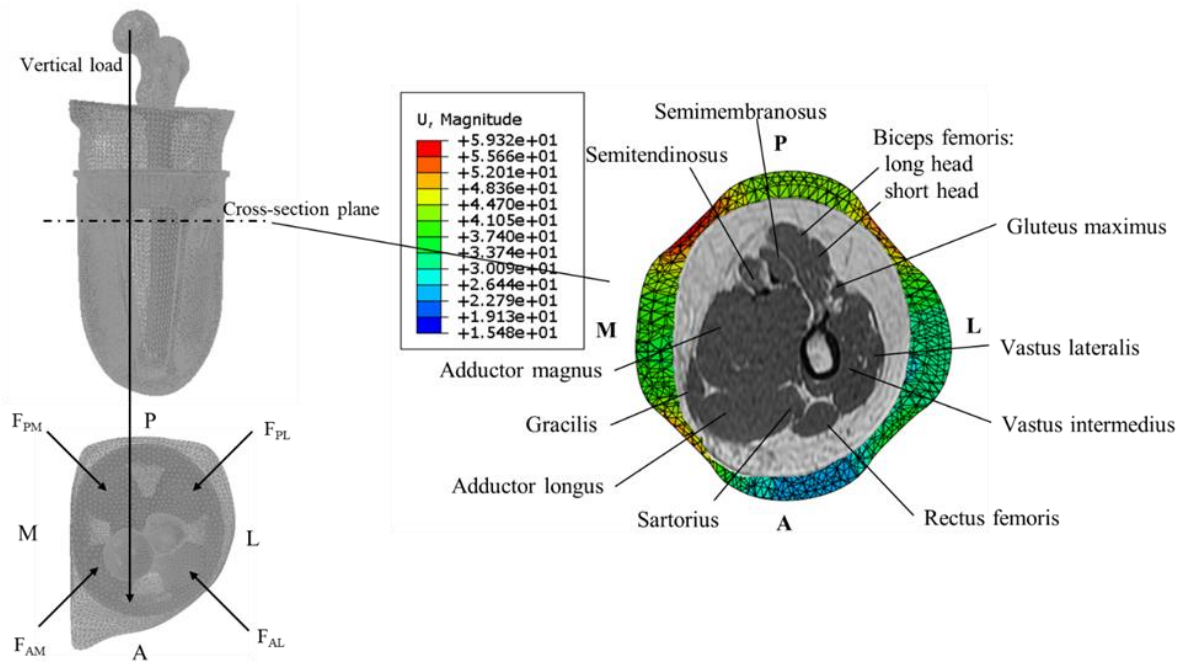

Figure 6. 1 Top and cross-section view of the FE model

6.2 Von Mises stress on the residual limb

The von Mises stress distribution pattern illustrated that the stress was distributed along the middle portion of the anterior-lateral compression area of the residual limb. For the other three compression areas, the stresses were concentrated at the upper portion. To improve the CRS socket design, the von Mises and normal stresses should be evenly distributed to enhance comfort. From the baseline of the inner CRS socket, the structure was depressed equally 15/10mm to achieve compression. With stress predicted, the socket structure should be modified to reduce the compression depth of upper parts of anterior-medial, posterior-medial, and posterior-lateral compression bars. Then the stresses on the upper part could be reduced for better comfort.

6.3 Silicone liner and coefficient of friction

By employing a simulated silicone liner, the pressure was reduced about 40%. The simulated liner was 3mm thick. However, most of the commercially available liners have 3mm thickness at the upper brim and 5mm or up to 7 mm thick at the bottom. The stress and pressure may be further reduced if we an actual liner will be applied.

The shear force was found approximately linear increased with the increase of the coefficient of friction, which agreed with Zhang and Mak's (1996) work on transtibial and transfemoral amputees finite element study. The stress may be further reduced if the coefficient of friction can be minimized.

The questionnaire reflected that the amputee did not has discomfort and was satisfied with the CRS socket. Clinical trial of longer duration should be conducted to examine the long-term effect of this socket design.

6.4 Limitation of this study

The pressure sensors for the experimental validation may have some dead cells, which cannot adequately evaluate the contact pressure. As the pressure was mostly concentrated at the proximal part of the residual limb, it did not influence much on the results of the validation.

In vivo, the joint reaction force was not vertical, and was three-dimensional (Figure 6.2) (Monk et al., 2013). The magnitude and direction of the forces were determined by the angle

of femur and muscles orientation. These parameters also vary among different persons. The load applied in the simulation was simplified as a vertical force.

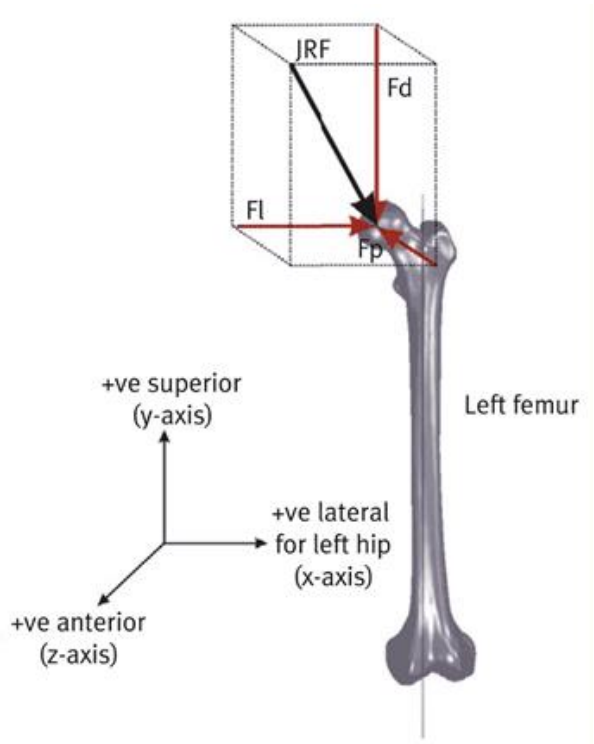

Figure 6. 2 The direction of actual load on the human femur in anatomic position (Monk et al., 2013)

CHAPTER 7 CONCLUSIONS AND FURTHER STUDY

This study examined the stress and strain distribution for a transfemoral amputee using a 15mm and 10mm compression CRS socket by the FE simulation. The CRS socket stabilizes the bone inside the soft tissue by further compressing the residual limb surface. However, additional compression induced stress and pressure may let patient experience pain and discomfort, especially when the skin condition is not good or sensitive to the pressure. The contributions of this study were that it illustrated stress and strain distribution for CRS socket with different compression depth, different coefficient of friction, with and without using a silicone liner. A good prosthetic socket should provide optimum stability control of residual limb but minimize the pressure exerted on it. As the CRS socket exerting more pressure on the residual limb, the socket configuration especially the compression bars have to be carefully considered.

The effect of a simulated 3mm silicone liner was also examined. A good CRS socket design can be achieved by adjusting the factors such as compression depth, the coefficient of friction and silicone liner when we have a better understanding of their effect. The pressure increased with the compression depth increase. Although the patient did not report any discomfort of the 15mm compression CRS socket, the study evaluated the static condition. During walking, the vertical load acting on the hip joint will increase several times of the body weight. The dynamic walking inducing higher pressure should be investigated to examine the long-term effect on the residual limb. Furthermore, the vascular circulation needs to be checked for the potential blockage of blood flow. By lowering the proximal brim of the prosthetic socket, the

patient’s hip range of motion will increase. This increased free motion of hip joint may allow a more neutral and symmetric gait. The motion analysis is required to compare this new approach with the traditional Quad and/or IRC socket.

Because of the high compression value of the CRS design, all the material properties were assumed to be linear elastic, homogeneous and isotropic to reduce the computational cost. The Young's modulus and Poisson’s ratio vary for skin and muscle groups with different structure and strength. In the future, the hyperelastic property of soft tissue should be considered.

In this study, the design of the CRS socket was based on the 3D reconstructed geometry of the residual limb. It has the advantage of the design of the CRS socket and easy assembly of the FE model. However, the compression value was obtained from the patient experiment. Further study should focus on the establishment of a correlation of soft tissue property and compression value. Once the correlation has been found and approved by larger sample size, the simulation and construction of CRS socket can include the corresponding tissue property of individual amputee. The appropriate socket would be produced after the FE simulation. The fabrication process can be enhanced and minimize the refit of the prosthesis.

References:

Al-Fakih, E., Abu Osman, N. A., & Mahamd Adikan, F. R. (2012). The use of fiber Bragg grating sensors in biomechanics and rehabilitation applications: the state-of-the-art and ongoing research topics. *Sensors, 12*(10), 12890-12926.

Al-Fakih, E. A., Osman, N. A. A., Eshraghi, A., & Adikan, F. R. M. (2013). The capability of fiber Bragg grating sensors to measure amputees' trans-tibial stump/socket interface pressures. *Sensors, 13*(8), 10348-10357.

Alley, R. D., Walley Williams III, T., Albuquerque, M., & Altobelli, D. E. (2011). Prosthetic sockets stabilized by alternating areas of tissue compression and release. *Journal of Rehabilitation Research and Development, 48*(6), 679.

Alley, R. D., Walley Williams III, T. (2012). Method for use of a compression stabilized prosthetic socket interface. *Google Patents*.

Backus, B. (2005). Problems in lower limb socket fit and present clinical solutions. *The Academy Today, 1*, 8-9.

Bakalima, G. (1966). Experiences with the total-contact prosthesis. *Artificial Limbs, 11*(1), 51-57.

Beil, T. L., Street, G. M., & Covey, S. J. (2002). Interface pressures during ambulation using suction and vacuum-assisted prosthetic sockets. *Journal of Rehabilitation Research* and Development, 39(6), 693.

Boone, D. A., & Coleman, K. L. (2006). Use of the prosthesis evaluation questionnaire (PEQ). *JPO: Journal of Prosthetics and Orthotics*, 18(6), 68-P79.

Branemark, R., Branemark, P., Rydevik, B., & Myers, R. R. (2001). Osseointegration in skeletal reconstruction and rehabilitation: a review. *Journal of Rehabilitation Research and Development, 38*(2), 175.

Buckley, J. G., Spence, W. D., & Solomonidis, S. E. (1997). Energy cost of walking: comparison of "intelligent prosthesis" with conventional mechanism. *Archives of Physical Medicine and Rehabilitation, 78*(3), 330-333.

Bui, K. M., Raugi, G. J., Nguyen, V. Q. & Reiber, G. E. (2009). Skin problems in individuals with lower-limb loss: Literature review and proposed classification system. *Journal of Rehabilitation Research and Development, 46*(9), 1085-1090.

Cook, R. D. (1995). *Finite element modeling for stress analysis*: Wiley.Colombo, G., Morotti, R., & Rizzi, C. (2014). FE analysis of contact between residual limb and socket during simulation of amputee motion. *Computer-Aided Design and Application*, 11(4): 381-388.

Condie, E., Scott, H., & Treweek, S. (2006). Lower limb prosthetic outcome measures: a review of the literature 1995 to 2005. *JPO: Journal of Prosthetics and Orthotics,* 18(6), 13-P45.

Culter, T. J. (2017). Rehabilitation of an individual with transfemoral amputation combing aquatic ambulation with prosthetic socket incorporating high-fedelity skeletal caputure. *Journal of Prosthetics and Orthotics,* 29: 206-212.

Dillingham, T. R., Pezzin, L. E., & MacKenzie, E. J. (2002). Limb amputation and limb deficiency: epidemiology and recent trends in the United States. *South Med J, 95*(8), 875-884.

Dudek, N. L., Marks, M. B., & Marshall, S.C. (2006). Skin problems in an amputee clinic. *American Journal of Physical Medicine & Rehabilitation, 85*(5), 424-429.

Dudek, N. L., Marks, M. B., Marshall, S. C., & Chardon, J. P. (2005). Dermatologic conditions associated with use of a lower-extremity prosthesis. *Archives of Physical Medicine and Rehabilitation, 86*(4), 659-663.

Eberhart, H. D., & McKennon, J. C. (1954). Suction-socket suspension of the above-knee prosthesis. *Human limbs and their substitutes*.

Ephraim, P. L., Dillingham, T. R., Sector, M., Pezzin, L. E., & MacKenzie, E. J. (2003). Epidemiology of limb loss and congenital limb deficiency: a review of the literature. *Archives of Physical Medicine and Rehabilitation, 84*(5), 747-761.

Fairley, M. (2004). MAS socket: a transfemoral revolution. *O&P Journal*, 6.

Gallagher, P., Franchignoni, F., Giordano, A., & MacLachlan, M. (2010). Trinity amputation and prosthesis experience scales: a psychometric assessment using classical test theory and rasch analysis. *American Journal of Physical Medicine & Rehabilitation,* 89(6), 487-496.

Gallagher, P., & MacLachlan, M. (2004). The Trinity amputation and prosthesis experience scales and quality of life in people with lower-limb amputation 1. *Archives of Physical Medicine and Rehabilitation*, 85(5), 730-736.

Gailey, R., Lawrence, D., Burditt, C., Spyropoulos, P., Newell, C., & Nash, M. (1993). The CAT-CAM socket and quadrilateral socket: a comparison of energy cost during ambulation. *Prosthetics and Orthotics International*, 17(2), 95-100.

Gauthier-Gagnon, C., & Grisé, M. C. (1994). Prosthetic profile of the amputee questionnaire: validity and reliability. *Archives of Physical Medicine and Rehabilitation*, 75(12), 1309-1314.

Gibson, J. (2001). Lower limb amputation. *Nursing Standard*, *15*(28), 47-52.

Gottschalk, F. (1992). Transfemoral amputation: Surgical procedures. In Bowker JH & M. Jw (Eds.), *Atlas of limb prosthetics: Surgical, prosthetic, and rehabilitation principles. 2nd ed. St Louis (MI): Mosby Year Book.*

Gottschalk, F. A., Kourosh, S., Stills, M., McClellan, B., & Roberts, J. (1989). Does Socket Configuration Influence the Position of the Femur in Above-Knee Amputation? *Journal of Prosthetics and Orthotics*, *2*(1), 94.

Gottschalk, F. A., & Stills, M. (1994). The biomechanics of trans-femoral amputation. *Prosthetics and Orthotics International*, *18*(1), 12-17.

Guggenberger, R., Pfirrmann, C. W., Koch, P. P., & Buck, F. M. (2014). Assessment of lower limb length and alignment by biplanar linear radiography: comparison with supine CT and upright full-length radiography. *American Journal of Roentgenology*, 202(2), 161-167.

Hagberg, K., Haggstrom, E., Uden, M., & Brånemark, R., (2005). Socket versus bone-achored trans-femoral prostheses: hip range of motion and sitting comfort. *Prosthet Orthot Int*, 29: 153-163.

Hagberg, K., Hansson, E., & Brånemark, R. (2014). Outcome of percutaneous osseointegrated prostheses for patients with unilateral transfemoral amputation at two-year follow-up. *Archives of Physical Medicine and Rehabilitation*, *95*(11), 2120-2127.

Hall, C. B. (1964). Prosthetic socket shape as related to anatomy in lower extremity amputees. *Clinical Orthopaedics and Related Research*, *37*, 32-46.

Hayes, W., Keer, L., Herrmann, G., & Mockros, L. (1972). A mathematical analysis for indentation tests of articular cartilage. *Journal of Biomechanics, 5*(5), 541-551.

Heim, M., Wershavski, M., Zwas, S. T., Siev-Ner, I., Nadvorna, H., & Azaria, M. (1997). Silicone suspension of external prostheses: a new era in artificial limb usage. *The Journal of Bone and Joint Surgery, 79*(4), 638-640.

Horgan, O., & MacLachlan, M. (2004). Psychosocial adjustment to lower-limb amputation: a review. *Disability and Rehabilitation, 26*(14-15), 837-850.

Huang, C., Jackson, J., Moore, N., Fine, P., Kuhlemeier, K., Traugh, G., & Saunders, P. (1979). Amputation: energy cost of ambulation. *Archives of Physical Medicine and Rehabilitation, 60*(1), 18-24.

Kahle, J. T., Klenow, T. D., Sampson, W. J., & Highsmith, M. J. (2016). The effect of transfemoral interface design on gait speed and risk of falls. *Technology and innovation, 18*(2-3), 167.

Kanellos, G. T., Tsiokos, D., Pleros, N., Childs, P., & Pissadakis, S. (2011). Enhanced durability fbg-based sensor pads for biomedical applications as human-machine interface surfaces. *BioPhotonics*, 2011 International Workshop .

Kapp, S. (1999). Suspension systems for prostheses. *Clinical Orthopaedics and Related Research, 361*, 55-62.

Klasson, B. (1985). Computer aided design, computer aided manufacture and other computer aids in prosthetics and orthotics. *Prosthetics and Orthotics International, 9*(1), 3-11.

Klotz, R., Colobert, B., Botino, M., & Permentiers, I. (2011). Influence of different types of socket on the range of motion of hip joint by the transfemoral amputee. *Ann Phys Rehabil Med*, 54: 399-410.

Klute, G. K., Glaister, B. C., & Berge, J. S. (2010). Prosthetic liners for lower limb amputees: a review of the literature. *Prosthetics and Orthotics International, 34*(2), 146-153.

Kumbha, K. R., & Kamarthi, K. M. (2016). Incidence of amputation in emergency. J. Evid. Based Med, 3(63), 2349-2562.

Lacroix, D., & Patiño, J. F. R. (2011). Finite element analysis of donning procedure of a prosthetic transfemoral socket. *Annals of Biomedical Engineering, 39*(12), 2972-2983.

Lee, W. C., Zhang, M., & Mak, A. F. (2005). Regional differences in pain threshold and tolerance of the transtibial residual limb: including the effects of age and interface material. *Archives of Physical Medicine and Rehabilitation, 86*(4), 641-649.

Legro, M. W., Reiber, G. D., Smith, D. G., Del Aguila, M., Larsen, J., & Boone, D. (1998). Prosthesis evaluation questionnaire for persons with lower limb amputations: assessing prosthesis-related quality of life. *Archives of Physical Medicine and Rehabilitation*, 79(8), 931-938.

Lenze, J. F., & Del Rossi, J. (1994). Suction socket for artificial limb: Google Patents.

Long, I. A. (1975). Allowing normal adduction of femur in above-knee amputations. *Orthotics and Prosthetics, 29*(4), 53-54.

Long, I. A. (1985). Normal shape-normal alignment (NSNA) above-knee prosthesis. *Clinical Prosthetics and Orthotics, 9*(4), 9-14.

Lundberg, M., Hagberg, K., & Bullington, J. (2011). My prosthesis as a part of me: a qualitative analysis of living with an osseointegrated prosthetic limb. *Prosthetics and Orthotics International, 35*(2), 207-214.

Lyon, C. C..,Kulkani, J., Zimerson, E., Van Ross, E., & Beck, M. H.. (2000). Skin disorders in amputees. *Journal of the American Academy of Dermatology, 42*(3), 501-507.

Mak, A. F., Zhang, M., & Boone, D. A. (2001). State-of-the-art research in lower-limb prosthetic biomechanics-socket interface: A review. *Journal of Rehabilitation Research and Development, 38*(2), 161.

Marshall, C.., Barakat, T.,Stansby, G. (2016). Amputation and rehabilitation. *Surgery (Oxford), 34*(4), 188-191.

Maurer, J., Ronsky, J., Loitz-Ramage, B., Andersen, M., Zernicke, R., & Harder, J. (2003). *Prosthetic socket interface pressures: Customized calibration technique for the TEKSCAN F-socket system.* Paper presented at the Summer Bioengineering Conference. Sonesta Beach Resort in Key Biscayne, Florida, USA.

Meulenbelt, H. E., Geertzen, J. H., Jonkman, M. F., & Dijkstrad, P. U. (2011). Skin problems of the stump in lower limb amputees: 1. A clinical study. *Acta Dermato-Venereologica, 91*(2), 173-177.

Monk, A., Simpson, D., Riley, N. D., Murray, D., & Gill, H. (2013). Biomechanics in orthopaedics: considerations of the lower limb. *Surgery (Oxford), 31*(9), 445-451.

Moxey, P., Hofman, D., Hinchliffe, R., Jones, K., Thompson, M., & Holt, P. (2010). Epidemiological study of lower limb amputation in England between 2003 and 2008. *British Journal of Surgery, 97*(9), 1348-1353. `

Newcombe, L., Dewar, M., Blunn, G. W.,& Fromme, P. (2013). Effect of amputation level on the stress transferred to the femur by an artificial limb directly attached to the bone.*Medical Engineering & Physics, 35*(12), 1744-1753.

Nielsen, C. C. (1991). A Survey of Amputees: Functional Level and Life Satisfaction, Information Needs, and the Prosthetist's Role. *Journal of Prosthetics and Orthotics, 3*(3), 125-129.

Ortiz, M., Rodolfo Marlo Vazquez. (2013). Method of making an anatomical socket: Google Patents.

Pabmelee, D. D. (1863). Improvement in artificial legs: Google Patents.

Paterno, L., Ibrabimi, M., Gruppioni, E., Menciassi, A., & Ricotti, L. (2018). Socket for limb prostheses: a review of existing technologies and open challenges. IEEE Trans Biomed Eng, 65: 1-15.

Pike, A. (2002). A new Concept in Above Knee Socket Design. *O&P Journal, 11*.

Portnoy, S., Yarnitzky, G., Yizhar, Z., Kristal, A., Oppenheim, U., Siev-Ner, I., & Gefen, A. (2007). Real-time patient-specific finite element analysis of internal stresses in the soft tissues of a residual limb: a new tool for prosthetic fitting. *Annals of Biomedical Engineering, 35*(1), 120-135.

Portnoy, S., Yizhar, Z., Shabshin, N., Itzchak, Y., Kristal, A., Dotan-Marom, Y., . . . Gefen, A. (2008). Internal mechanical conditions in the soft tissues of a residual limb of a trans-tibial amputee. *Journal of Biomechanics, 41*(9), 1897-1909.

Prendergast, P. (1997). Finite element models in tissue mechanics and orthopaedic implant design. *Clinical Biomechanics, 12*(6), 343-366.

Pritham, C. H. (1988). Workshop On Teaching Materials for Above-Knee Socket Variants. *Journal of Prosthetics and Orthotics, 1*(1), 50-67.

Pritham, C. H. (1999). Biomechanics and shape of the above-knee socket considered in light of the ischial containment concept. *Prosthet Orthot Int,* 14: 9-21

Radcliffe, C. W. (1955). Functional considerations in the fitting of above-knee prostheses. *Artificial Limb,* 2(1), 35-60.

Ramírez, J. F., & Vélez, J. A. (2012). Incidence of the boundary condition between bone and soft tissue in a finite element model of a transfemoral amputee. *Prosthetics and Orthotics International, 36*(4), 405-414.

Resnik, L., Patel, T., Cooney, S. G., Crisco, J. J., & Fantini, C. (2014). Comparison of transhumeral socket designs utilizing patient assessment and in vivo skeletal and socket motion tracking: a case study. *Disability and Rehabilitation: Assistive Technology*, 11(5), 423-432.

Reynolds, D., & Lord, M. (1992). Interface load analysis for computer-aided design of below-knee prosthetic sockets. *Medical and Biological Engineering and Computing, 30*(4), 419-426.

Robinovitch, S. N., McMahon, T. A., & Hayes, W. C. (1995). Force attenuation in trochanteric soft tissues during impact from a fall. *J Orthop Res, 13*(6), 956-962.

Sabolich, J. (1985). Contoured adducted trochanteric-controlled alignment method (CAT-CAM): introduction and basic principles. *Clinic Prosthetics and Orthotics, 9*(4), 15-26

Schmalz, T., Blumentritt, S., & Jarasch, R. (2002). Energy expenditure and biomechanical characteristics of lower limb amputee gait: the influence of prosthetic alignment and different prosthetic components. *Gait Posture,* 16(3), 255-263.

Schofield, J. S., Schoepp, K. R., Williams, H. E., Carey, J. P., Marasco, P. D., & Hebert, J. S. (2017). Characterization of interfacial socket pressure in transhumeral prostheses: A case series. *PloS one,* 12(6), e0178517.

Schuch C.M. (1987). Report from: international workshop on above-knee fitting and alignment techniques. *Clinical Prosthetics and Orthotics,* 12: 81-98.

Schuch, C. M. , & Charles H. (1999). Current transfemoral sockets. *Clinical orthopaedics and related research, 361*, 48-54.

Sheehan, T. P.., & George C. (2014). Impact of Limb Loss in the United States. *Physical Medicine and Rehabilitation Clinics of North America, 25*(1), 9-28.

Shurr, D. G., & Michael, J. W. (2002). *Prosthetics and Orthotics* (2nd ed.). Upper Saddle River, N.J: Prentice Hall.

Silver-Thorn, M. B. (1996). Parametric analysis using the finite element method to investigate prosthetic interface stresses for persons with trans-tibial amputation. *Journal of Rehabilitation Research and Development, 33*(3), 227.

Smith, D. G., Ehde, D. M., Legro, M. W., Reiber, G. E., Del Aguila, M., & Boone, D. A. (1999). Phantom limb, residual limb, and back pain after lower extremity amputations. *Clinical Orthopaedics and Related Research, 361,* 29-38.

Smith, D. G., Michael, J. W., Bowker, J. H. (2004). Atlas of amputations and limb deficiencies: surgical, prosthetic, and rehabilitation principles, 3rd ed. Rosemont, IL: American Academy of Orthopaedic Surgeons Rosemont.

Steege, J., Schnur, D., Van Vorhis, R., & Rovick, J. (1987). Finite element analysis as a method of pressure prediction at the below-knee socket interface. *Paper presented at the Proceedings of RESNA 10th Annual Conference,* California.

Sullivan, J., Uden, M., Robinson, K., & Sooriakumaran, S. (2003). Rehabilitation of the trans–femoral amputee with an osseointegrated prosthesis: The United Kingdom experience. *Prosthetics and Orthotics International, 27*(2), 114-120.

Taddei, F., Schileo, E., Helgason, B., Cristofolini, L., & Viceconti, M. (2007). The material mapping strategy influences the accuracy of CT-based finite element models of bones: an evaluation against experimental measurements. *Medical Engineering & Physics, 29*(9), 973-979.

Traballesi, M., Delussu, A. S., Averna, T., Pellegrini, R., Paradisi, F., & Brunelli, S. (2011) Energy cost of walking in transfemoral amputees: comparison between Marlo Anatomical Socket and ischial containment socket. *Gait Posture,* 34: 270-274.

Trower, T. A. (2006). Changes in lower extremity prosthetic practice. *Phys Med Rehabil Clin N Am,* 17: 23-30.

Turney, B. K., SJ; Walker, RT; Loftus, IM. (2001). Amputations: no longer the end of the road. *Journal of the Royal College of Surgeons of Edinburgh, 46*(5), 271-273.

Uustal, H. M., Robert H. (2014). Pain Issues and Treatment of the Person with an Amputation. *Physical Medicine and Rehabilitation Clinics of North America, 25*(1), 45-52.

Van de Meent, H.., Maria T., Frölke,J. P. (2013). Walking Ability and Quality of Life in Subjects With Transfemoral Amputation: A Comparison of Osseointegration With Socket Prostheses. *Archives of Physical Medicine and Rehabilitation, 94*(11), 2174-2178.

Velez, Z. J., Bustamante, G. L., Villarraga, O. J. (2015). Relation between residual limb length and stress distribution over stump for transfemoral amputees. Revista EIA, 12(23): 107-115.

Versluys, R., Pieter, B., Van Damme, M., Desomer, A., Van Ham, R., & Lefeber, D. (2009). Prosthetic feet: State-of-the-art review and the importance of mimicking human ankle-foot biomechanics. *Disability and Rehabilitation: Assistive Technology, 4*(2), 65-75.

Wang, J., Thornton, J. C., Russell, M., Burastero, S., Heymsfield, S., & Pierson, R. (1994). Asians have lower body mass index (BMI) but higher percent body fat than do whites: comparisons of anthropometric measurements. *The American journal of clinical nutrition, 60*(1), 23-28.

Waters, R., Perry, J., Antonelli, D., & Hislop, H. (1976). Energy cost of walking of amputees: the influence of level of amputation. *The Journal of Bone and Joint Surgery, 58*(1), 42-46.

Waters, R. L., & Mulroy, S. (1999). The energy expenditure of normal and pathologic gait. *Gait & Posture, 9*(3), 207-231.

Wewers, M. E., & Lowe, N. K. (1990). A critical review of visual analogue scales in the measurement of clinical phenomena. *Research in nursing & health,* 13(4), 227-236.

Yoo, S. (2014). Complications Following an Amputation. *Physical Medicine and Rehabilitation Clinics of North America, 25*(1), 169-178.

Zhang, L., Zhu, M., Shen, L., & Zheng, F. (2013). Finite element analysis of the contact interface between trans-femoral stump and prosthetic socket. *Paper presented at the 2013 35th Annual International Conference of the IEEE Engineering in Medicine and Biology Society (EMBC).*

Zhang, M., & Mak, A. F(1996). A finite element analysis of the load transfer between an above-knee residual limb and its prosthetic socket-roles of interface friction and distal-end boundary conditions. *Rehabilitation Engineering, IEEE Transactions on, 4*(4), 337-346.

Zhang, M.,Mak, A. F., & Roberts, V. (1998). Finite element modelling of a residual lower-limb in a prosthetic socket: a survey of the development in the first decade. *Medical Engineering & Physics, 20*(5), 360-373.

Zhang, M., & Roberts, C. (1970). Development of a nonlinear finite element model for analysis of stump/socket interface stresses in below-knee amputee. *WIT Transactions on Biomedicine and Health, 1*.

Ziegler-Graham, K., MacKenzie, E. J., Ephraim, P. L., Travison, T. G., Brookmeyer, R.. (2008). Estimating the prevalence of limb loss in the United States: 2005 to 2050. Arch Phys Med Rehabil, 89(3), 422-429.

Zink, A., Szeimies., & Hagedorn, H. (2000). Ancient egyptian prosthesis of the big toe. *The Lancet*, 356(9248), 2176-2179.

Appendices

Appendix I: MRI Scanning Preparation

One transfemoral amputee's MR image is required for this finite element study. The scanning duration is around half an hour. In the MRI scanning, the residual limb including the hip joint will be captured. The patient is positioned in a supine lying position and wearing an unmodified plaster cast to prevent deformation of the soft tissue due to the gravity.

The detailed information on preparation and positioning the patient for MRI shows below:

Prepare the unmodified plaster cast

One negative cast is made for the patient's residual limb using plaster bandage. During the casting, the patient is in the standing position, with the sound side supported by the casting stand. The prosthetist firmly warps the plaster of the bandage around the patient's residual limb. After wrapping, the patient keeps his residual limb in the adducted position until the plaster set, and no modification of the plaster cast is needed to keep the residual limb's origin shape.

The prosthetist marks the alignment line in the frontal and sagittal plane before taking off the cast from the patient (Figure 8. 1).

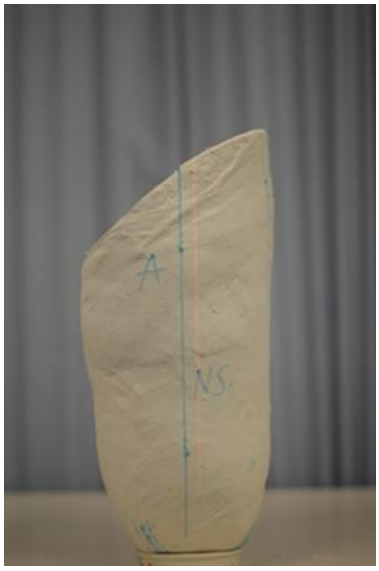

Figure 8. 1 The unmodified plaster cast

Plan and instruct the patient's position before the real MRI scanning.

The patient is standing in front of the scanning table with his buttock supported by the scanning table. The researcher puts the cast sock/stockings on subject' residual limb and the distal end of sock beyond the residual limb about 10cm (Figure 8.2 Left).

The researcher holds the negative cast in front of the patient and put the sock through the hole at the distal end of the cast. The researcher uses one hand to push up, and stable the cast, the other hand slowly pulls the distal end of the sock from the anterior, lateral, posterior, and medial side until the distal end of residual limb fully contact with the cast (Figure 8.2 right);

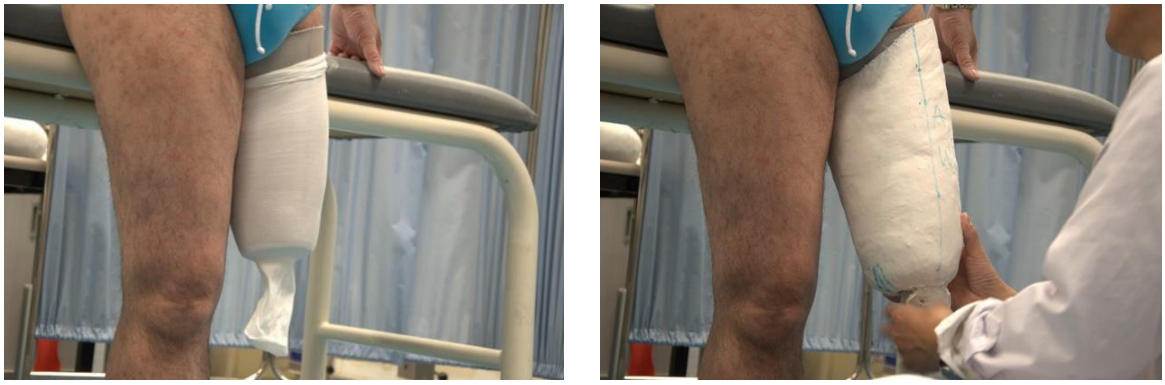

Figure 8. 2 Left, the patient is wearing the socks on the residual limb; right, the researcher dons the cast on the patient residual limb.

The researcher puts the sewing strap on the negative cast and wraps the waist belt around the shoulder. Once the cast is well fitted, the researcher tightens the belt.

The patient sits on the edge of the scanning table and then moves his buttock and body in the middle of the scanning table. The patient is supine lying on the bench with the hip in the neutral position. The sound side knee is extended. The residual limb is aligned with the plumb reference line horizontal with the ground, support the residual limb using the towel to adjust the alignment whenever it is necessary.

Double check the suspension of the cast to make sure there is no relative distal sliding of the cast with soft tissue. The patient is supine lying on the gantry with the hip and knee joint fully extended. Ankles are slightly apart and internally rotated until toes pointing upwards (Guggenberger et al., 2014)

To start the MRI scanning (Figure 8.3).

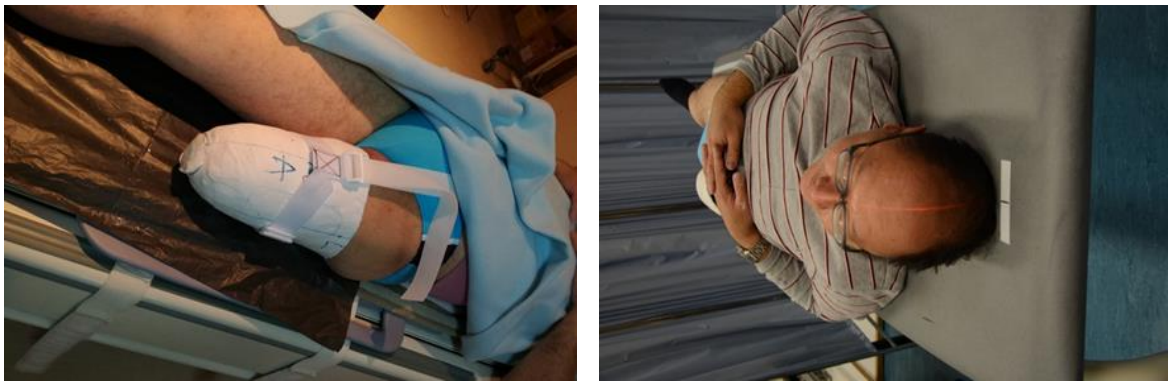

Figure 8. 3 left, the patient is ready for MRI scanning; right, checking the patient position

Appendix II: CRS Prosthetic Socket Evaluation Questionnaire

1. How do you think about the fit of socket, please tick as appropriate:

☐1 ☐2 ☐3 ☐4 ☐5

5 scales: 1 terrible, 2 unsatisfactory, 3 fair, 4good, 5 excellent

2. How do you think about the weight, please tick:

☐1 ☐2 ☐3 ☐4 ☐5

5 scales: 1 terrible, 2 unsatisfactory, 3 fair, 4good, 5 excellent

3. How do you think about standing comfort, please tick

☐1 ☐2 ☐3 ☐4 ☐5

5 scales: 1 poor, 2 unsatisfactory, 3 fair, 4good, 5 excellent

4. How do you think about sitting comfort, please tick:

☐1 ☐2 ☐3 ☐4 ☐5

5 scales: 1 poor, 2 unsatisfactory, 3 fair, 4good, 5 excellent

5. Do you feel any pain on the socket, please tick:

☐1 ☐2 ☐3 ☐4 ☐5

5 scales: 1 severe pain, 2 painful, 3 no pain, 4 comfortable, 5 excellent

If there is any, please write down the location: _____

6. How do you think about the suction of the socket, please tick:

☐1 ☐2 ☐3 ☐4 ☐5

5 scales: 1 very loose, 2 loose, 3 fair, 4 good, 5 excellent

7. How do you think about doffing of the prosthesis, please tick:

☐1 ☐2 ☐3 ☐4 ☐5

5 scales: 1 terrible, 2 unsatisfactory, 3 fair, 4good, 5 excellent

8. How do you think about donning of the prosthesis, please tick:

☐1 ☐2 ☐3 ☐4 ☐5

5 scales: 1 poor, 2 unsatisfactory, 3 fair, 4good, 5 excellent

9. What is the overall feeling on the residual limb, please tick:

☐1 ☐2 ☐3 ☐4 ☐5

5 scales: 1 terrible, 2 unsatisfactory, 3 fair, 4good, 5 excellent

10. Please write down on the below if you have any comments:

_____

_____

Appendix III: Information sheet in English

THE HONG KONG
POLYTECHNIC UNIVERSITY
香港理工大學

INFORMATION SHEET

Finite Element Modelling for Evaluation of Compression/Release Stabilized Transfemoral Prosthetic Socket

You are invited to participate in a study conducted by Meng Zhaojian, who is a post-graduate student of the Department of Interdisciplinary Division of Biomedical Engineering in The Hong Kong Polytechnic University. The project has been approved by the Human Subjects Ethics Sub-committee (HSESC) (or its Delegate) of The Hong Kong Polytechnic University (HSESC Reference Number: XXX).

The aim of this study is to evaluate the compression/release stabilized transfemoral prosthetic socket by employing the finite element modeling method. The study will involve completing a questionnaire, which will take you about five minutes. You will then be asked to take part in a procedure to investigate MRI. There are two stages: First. Your residual limb will be taken by MRI equipment, and it is used for building the FE model. An unrectified cast will be made for you to maintain the geometry of residual limb during the MRI scanning. Second, your residual limb will be wrapped by plastic plaster to form a negative impression. The casting is used for making CRS socket. you will then wear this CRS designed prosthesis to walk. The interfacial pressure between the residual limb and socket will be recorded by pressure sensor inserted. Meanwhile, gait parameters will be collected by Vicon system. it is hoped the FEM simulation result will help Prosthetist-Orthotist (PO) to have a better understanding of CRS design. The predicted stress and strain on the residual limb will guide the PO design the CRS socket to make a most suitable and comfortable transfemoral prosthetic socket for the patient. The fitting and re-fitting times for amputees could be reduced.

The testing should not result in any undue discomfort. You may feel tired when we are taking the cast (around half an hour) and data collection during walking. The rest will be arranged between each trail as well as when you think it is needed. Photos and videos will be taken during the research. All information related to you will remain confidential and will be identifiable by codes only known to the researcher.

You have every right to withdraw from the study before or during the measurement without penalty of any kind. The whole investigation will take about 2 hours.

If you would like to obtain more information about this study, please contact Mr. Meng Zhaojian (tel. no.: 6633 / email: mecca.meng@

If you have any complaints about the conduct of this research study, please do not hesitate to contact Miss Cherrie Mok, Secretary of the Human Subjects Ethics Sub-Committee of The Hong Kong Polytechnic University in writing (c/o Research Office of the University) stating clearly the responsible person and department of this study as well as the HSESC Reference Number.

Thank you for your interest in participating in this study.

Principal Investigator: Dr. Aaron K.L. Leung

Hung Hom Kowloon Hong Kong 香港 九龍 紅磡
Tel 電話 (852) 2766 5111 Fax 傳真 (852) 2784 3374
Email 電郵 polyu@polyu.edu.hk
Website 網址 www.polyu.edu.hk

Appendix IV: Information sheet in Chinese

THE HONG KONG POLYTECHNIC UNIVERSITY
香港理工大學

研究信息表

受壓/釋放式大腿義肢接受腔的有限元分析

您被邀請參加由香港理工大學生物醫學工程學系研究員孟昭建設計的受壓/釋放式大腿義肢接受腔的有限元分析。該研究已取得香港理工大學倫理委員會的許可。倫理審查審批編號：XXX)

該研究的目的是運用有限元方法分析受壓/釋放式大腿義肢接受腔作用于殘肢上應力和應變。您將有一份約 10 分鐘的問卷填寫。研究分為兩個階段。你會被邀請參加一次大腿殘肢的核磁共振（MRI）掃描，該影響將會用於有限元的建模分析。在進行掃描時，您的殘肢上將會佩戴一石膏綳带製成的支具已保持殘肢的幾何形狀。第二階段，從您的殘肢上用石膏繃帶取一陰型模具用以製作受壓/釋放式大腿義肢接受腔。之後您會穿戴受壓/釋放式大腿義肢在實驗室進行步行實驗。殘肢上的受力情況將會被置於殘肢表面和接受腔之間的壓力傳感器所記錄，同時您的步態信息也會採集到步態分析系統（Vicon）上面。

是項研究不會引起您的不適。您可能會感到體力負擔當我們在給您殘肢用石膏繃帶取型時（約半小時）。實驗會在適當或者您認為需要時安排休息以保持體力。在研究期間會有影像和視頻資料記錄，但您的個人資料會嚴格保密，只有研究人員可以提取。

您有權利在任何時間提出退出此項研究，不會有任何責任。整個調查時間大約 2 小時。

如您需要了解更多信息，可隨時電話：6655　　或郵件：mecca.meng@
聯繫研究員孟昭建。

如您對研究有質疑，請聯繫 Cherrie Mok，香港理工大學倫理委員會委員。

感謝您參與此次研究

首席研究员
梁锦伦博士

Hung Hom Kowloon Hong Kong 香港 九龍 紅磡
Tel 電話 (852) 2766 5111 Fax 傳真 (852) 2784 3374
Email 電郵 polyu@polyu.edu.hk
Website 網址 www.polyu.edu.hk

Appendix V: Consent form in English

THE HONG KONG POLYTECHNIC UNIVERSITY
香港理工大學

CONSENT TO PARTICIPATE IN RESEARCH

Finite Element Modelling for Evaluation of Compression/Release Stabilized Transfemoral Prosthetic Socket

I _____ hereby consent to participate in the captioned research conducted by Meng Zhaojian a research student at Biomedical Engineering Department, The Hong Kong Polytechnic University.

I understand that information obtained from this research may be used in future research and published. However, my right to privacy will be retained, i.e. my personal details will not be revealed.

The procedure as set out in the attached information sheet has been fully explained. I understand the benefit and risks involved. My participation in the project is voluntary.

I acknowledge that I have the right to question any part of the procedure and can withdraw at any time without penalty of any kind.

Name of participant _____

If you have any question about this experiment, please feel free to contact Mr. Meng Zhaojian by phone: 6633 or Email: meccameng@

Signature of participant _____

Name of Parent or Guardian (if applicable)_____

Signature of Parent or Guardian (if applicable) _____

Name of researcher _____

Signature of research_____

Date _____

Hung Hom Kowloon Hong Kong 香港 九龍 紅磡
Tel 電話 (852) 2766 5111 Fax 傳真 (852) 2784 3374
Email 電郵 polyu@polyu.edu.hk
Website 網址 www.polyu.edu.hk

Appendix VI: Consent form in Chinese

THE HONG KONG POLYTECHNIC UNIVERSITY
香港理工大學

參與研究同意書

受壓/釋放型大腿義肢接受腔的有限元分析

本人_____同意參與由香港理工大學生物醫學工程系孟昭建開展的上述研究。

本人知悉此研究所得的資料可能被用作日後的研究及發表，但本人的私隱權利將得以保留，即本人的個人資料不會被公開。

研究人員已向本人清楚解釋列在所附資料卡上的研究程序，本人明瞭當中涉及的利益及風險；本人自願參與研究項目。

本人知悉本人有權就程序的任何部分提出疑問，並有權隨時退出而不受任何懲處。

如您對此研究有任何問題，歡迎隨時通過電話或者電郵聯繫孟昭建。電話：6633
郵件：mecca.meng@

參與者姓名 _____
參與者簽署 _____
家長或監護人(如適用) 姓名 _____
家長或監護人(如適用) 簽署 _____
研究人員姓名 _____
研究人員簽署 _____
日期 _____

Hung Hom Kowloon Hong Kong 香港 九龍 紅磡
Tel 電話 (852) 2766 5111 Fax 傳真 (852) 2784 3374
Email 電郵 polyu@polyu.edu.hk
Website 網址 www.polyu.edu.hk

Appendix VII: Ethical approval

THE HONG KONG POLYTECHNIC UNIVERSITY
香港理工大學

To	Leung Kam Lun (Interdisciplinary Division of Biomedical Engineering)		
From	Sun Lei, Chair, Departmental Research Committee		
Email	lei.sun@	Date	21-Dec-2016

Application for Ethical Review for Teaching/Research Involving Human Subjects

I write to inform you that approval has been given to your application for human subjects ethics review of the following project for a period from 06-Jun-2016 to 30-Dec-2017:

Project Title:	Finite Element Modelling for Evaluation of Compression/Release Stabilized Transfemoral Prosthetic Socket
Department:	Interdisciplinary Division of Biomedical Engineering
Principal Investigator:	Leung Kam Lun
Project Start Date:	06-Jun-2016
Reference Number:	HSEARS20161011002

You will be held responsible for the ethical approval granted for the project and the ethical conduct of the personnel involved in the project. In the case of the Co-PI, if any, has also obtained ethical approval for the project, the Co-PI will also assume the responsibility in respect of the ethical approval (in relation to the areas of expertise of respective Co-PI in accordance with the stipulations given by the approving authority).

You are responsible for informing the Human Subjects Ethics Sub-committee in advance of any changes in the proposal or procedures which may affect the validity of this ethical approval.

Sun Lei

Chair

Departmental Research Committee